Redox Biology 86 (2025) 103830

Contents lists available at ScienceDirect

Redox Biology

journal homepage: www.elsevier.com/locate/redox

Selective inhibition of NOX2 after status epilepticus attenuates epileptogenesis and cognitive impairment: A sex-dependent study

Prince Kumar Singh [a], Shweta Maurya [a], Aseel Saadi [a], Taige Zhang [a], Andreas Lieb [b], Tawfeeq Shekh-Ahmad [a,*]

[a] The Institute for Drug Research, The School of Pharmacy, Faculty of Medicine, The Hebrew University of Jerusalem, Jerusalem, 91120, Israel
[b] Institute of Pharmacology, Medical University of Innsbruck, 6020, Innsbruck, Austria

ARTICLE INFO

Keywords:
GSK2795039
NADPH oxidase 2
Epileptogenesis
Kainic acid
Oxidative stress

ABSTRACT

Epilepsy, a chronic neurological disorder affecting approximately 1 % of the global population, is characterized by recurrent seizures that are often refractory to current antiseizure medications (ASMs). These pharmacotherapies predominantly suppress symptoms without intervening in the underlying pathophysiological cascade, which includes persistent oxidative stress and neuroinflammation, key drivers of epileptogenesis and pharmacoresistance. Among the primary enzymatic sources of reactive oxygen species (ROS), NADPH oxidase 2 (NOX2) has emerged as a central mediator of redox imbalance and neuroimmune activation in the brain. However, the sex-specific roles of NOX2 and its modulation as a therapeutic strategy remain largely unexplored.

Here, we investigated the therapeutic efficacy of GSK2795039, a selective and functionally active NOX2 inhibitor, in a kainic acid (KA)-induced status epilepticus (SE) rat model. We examined both acute and chronic outcomes of early NOX2 inhibition on oxidative stress, neuroinflammation, hippocampal neurodegeneration, and cognitive function, incorporating rigorous analysis of sex-dependent responses. Long-term effects on epileptogenesis were assessed using continuous 24/7 video-electrocorticographic (vECoG) monitoring.

Our results revealed that early GSK2795039 intervention significantly attenuated SE-induced oxidative damage, pro-inflammatory cytokine expression, and neuronal death, thereby mitigating the development of spontaneous recurrent seizures. Notably, male rats exhibited a more robust therapeutic response, including a marked reduction in seizure burden and improved cognitive performance, whereas females displayed a more modest response, suggesting the presence of compensatory or NOX2-independent antioxidant mechanisms.

These findings underscore the pivotal role of NOX2-derived ROS in driving epileptogenesis and highlight the translational potential of NOX2-targeted therapies. Importantly, our study revealed a clear sex divergence in therapeutic outcomes, reinforcing the necessity of integrating sex as a critical biological variable in preclinical and clinical strategies aimed at disease modification in epilepsy.

1. Introduction

Oxidative stress has emerged as a prominent player in the pathogenesis of epilepsy, where an imbalance between the level of reactive oxygen species (ROS) production and antioxidant defenses leads to cellular damage [1]. Oxidative stress and neuroinflammation have been observed in both experimental models and human epileptic tissue [2,3], which exacerbates each other in a self-perpetuating cycle of neuronal injury [1]. Brennan et al. (2009) demonstrated that NMDAR-induced superoxide production and subsequent neuronal death are primarily mediated by NADPH oxidase, not mitochondria [4]. Among all NOX isoforms, NOX2 is predominantly expressed in glia and neurons, and its activation is closely associated with various brain pathologies [5]. We and others have shown that NOX2 is upregulated following status epilepticus (SE), remains elevated for weeks in cortex and hippocampus, and is associated with oxidative stress, neuroinflammation and neuronal loss [6–8].

Neuroinflammation, characterized by microglial and astrocytic activation and the release of proinflammatory cytokines such as interleukin-1β (IL-1β), interleukin-6 (IL-6), and tumor necrosis factor-alpha (TNF-α), disrupt the blood-brain barrier, increases excitability, and promote the seizure propagation [9,10]. In contrast, anti-inflammatory

* Corresponding author.
E-mail address: Tawfeeq.Shekh-Ahmad@mail.huji.ac.il (T. Shekh-Ahmad).

https://doi.org/10.1016/j.redox.2025.103830
Received 23 June 2025; Received in revised form 11 August 2025; Accepted 18 August 2025
Available online 18 August 2025

cytokines like interleukin-10 (IL-10) play a neuroprotective role by counteracting the deleterious effects of pro-inflammatory mediators [11]. The crosstalk between oxidative stress and neuroinflammation, particularly via NOX2derived ROS, further exacerbates neuronal injury and seizure susceptibility [12–14]. Inhibition of NOX2 reduces microglial ROS production and associated neurotoxicity [15], making it a promising therapeutic target [16,17].

Sex differences in epilepsy are well-documented, indicating that males and females may exhibit distinct responses to both the underlying pathophysiological mechanisms of epilepsy and the treatments [18]. These differences are influenced by sex hormones, sex chromosome-linked genetic factors, epigenetic modifications, and their interactions with neural circuits, which together contribute to variations in seizure susceptibility, disease progression, and therapeutic outcomes [19,20]. Generally, males exhibit higher seizure susceptibility [19], while women experience unique epilepsy patterns, such as catamenial epilepsy, with seizure sensitivity fluctuating during puberty, pregnancy, and menopause [19]. Epilepsy associated psychiatric and cognitive comorbidities also varies with sex [18]. Sex hormones and their receptors such as membrane androgen receptor (mAR), influence oxidative stress signaling and neuroprotection, potentially driving sex differences in neurodegenerative diseases [21]. This underscores the interplay between sex hormones, and oxidative stress in epilepsy, and highlights the need for sex-specific research and treatment approaches. However, the role of NOX2 in sex-specific responses to SE and epileptogenesis remains unclear. Studies suggest that females exhibit lower levels of NOX expression and activity compared to males or ovariectomized females [22], and the level of ROS production and oxidative stress is also lower in females than in males [23]. Moreover, clinical and experimental investigations have revealed that females exhibit a higher antioxidant potential than males [24]. These studies highlight potential link between sex and oxidative stress, where females are less susceptible to oxidative stress or exhibit higher resistance to oxidative stress then males [25]. This observation raises the intriguing possibility that the contribution of NOX2-derived oxidative stress to epileptogenesis may be less pronounced in females, thereby potentially influencing the overall therapeutic response.

In this study, we specifically investigated the therapeutic potential of GSK2795039, a selective and functional NOX2 inhibitor, in the context of epilepsy. Our primary objective was to determine whether pharmacological inhibition of NOX2 with GSK2795039 could mitigate oxidative stress, neuroinflammation, and neuronal damage following status epilepticus, thereby reducing the risk and severity of epileptogenesis. Using a kainic acid-induced status epilepticus model of temporal lobe epilepsy, we assessed both acute and long-term outcomes, including seizure burden and cognitive deficits. A key focus was to explore sex-dependent differences in response to NOX2 inhibition. Recognizing distinct neuroinflammatory and neuroprotective mechanisms between males and females, we compared the efficacy of GSK2795039 across sexes by evaluating cytokine expression, neuronal injury, and behavioral outcomes. This sex-based approach addresses a critical gap in epilepsy research and aligns with calls for more inclusive, stratified analyses to enhance translational relevance. By combining targeted NOX2 inhibition with sex-specific analysis, our study aims to provide new insights into epileptogenesis and inform personalized therapeutic strategies that account for biological variability among patients.

2. Materials and methods

2.1. Animal model and surgical procedures

All animal experiments were conducted in accordance with the Association for Assessment and Accreditation of Laboratory Animal Care International and were approved by the Institutional Animal Care and Use Committee of the Hebrew University of Jerusalem (Approval No. MD-20-16,254-5). Naïve male and female Sprague–Dawley (SD) rats (150–175 gm) from the Hebrew University strain (Harlan, Jerusalem, Israel) were housed under controlled conditions (23 °C, 50–60 % humidity, 12-h light/dark cycle) with free access to food and water. All animals were acclimated for 7 days before the experiments.

2.1.1. Experimental grouping

This study was conducted in two phases. Fig. 1 highlights experimental grouping and animals' allocation for both phase: Total 96 animals (48 male & 48 female rats) were assigned into two experimental group: *Group 1:* Acute Post-SE Group (*Phase 1*); *Group 2*: Epileptogenesis Monitoring Group *(Phase 2)*.

Group 1 (left, no electrocorticography (ECoG) implantation surgery) was divided into the sham group (n = 20; 10 males, and 10 females), and the KA-induced SE group (n = 44, 22 males and 22 females) was further divided into the vehicle treatment group (n = 21; 10 males and 11 females of which 1 female died after SE) and the GSK-treated group (n = 23; 12 males and 11 females of which 2 males and 1 female died following SE). From each end terminal animals were split into two groups of 5–5 animals for biochemical analysis and perfusion for histochemical analysis.

Group 2 (right, surgery) underwent ECoG device implantation surgery (n = 32; 16 males, 16 females; out of them 1 male and 2 females failed to recover from surgery). All surviving animals underwent KA-SE induction (n = 29; 15 males and 14 females out of them 1 female and 2 male failed to survive KA-SE). All surviving animals were randomly allocated to either the vehicle group (n = 13; 7 males and 6 females) or GSK therapy group (n = 13; 6 males and 7 females) and received their respective treatment at a dose of 20 mg/kg/day (or equivalent volume of vehicle) for two week under video-ECoG (vECoG) surveillance (discussed below). After 2 weeks of therapy, the rats were subjected to continuous 24 × 7, vECoG monitoring for 12 weeks until the epileptogenesis phase was completed to assess the effect of therapy on epilepsy development in the sex cohort. The red highlighted numbers represent animals that failed to survive. At the end of the experiment, animals were sacrificed for biochemical investigation or perfusion for histochemical analysis to evaluate treatment effects at different stages of epilepsy development.

2.1.2. Animal surgery: implantation of ECoG transmitter

All naïve male and female rats were anesthetized with isoflurane (3 % for induction, 1.8–2.3 % for surgery; Terrell™, USP, Piramal Critical Care) and secured in a stereotaxic frame (Kopf, CA, USA). For analgesia, buprenorphine (0.2 mg/kg, s.c.; Rich Pharma) and Meloxicam (1 mg/kg, s.c.; Chanelle Pharma) were administered prior to surgeries. An ECoG transmitter (A3028E, Single channel, 512 Hz, Open-Source Instruments Inc.) was implanted subcutaneously to each rat with two subdural intracranial electrodes: the recording electrode above the right hippocampus (AP: 3 mm, ML: +2.5 mm) and the reference electrode in the contralateral hemisphere (AP: −6/7 mm, ML: +3.5 mm). The electrodes were secured using skull screws and tissue glue. Following surgery, the brain incision was sealed with dental cement, and the rats were administered with 3–5 ml of warmed Ringer's solution and amoxicillin (Betamox LA, 100 mg/kg) and returned to their home cages for recovery for next seven days.

2.1.3. Induction of status epilepticus

All male and female SD rats (175–200 g) were administered with kainic acid (5 mg/ml in 0.9 % saline; 10 mg/kg; *i.p.;* Hello-bio) hourly until class IV–V seizures were induced according to a modified Racine's scale [26]. KA administration was stop upon reaching class V seizures (rearing, forelimb clonus, and falling) or a cumulative dose of 45 mg/kg. Two hours after confirming status epilepticus (SE) with class V seizures, Diazepam (Assival®, 10 mg/kg, *i.p.*) was administered to terminate SE. All rats experiencing continuous motor seizures during the 2-hr post-SE period or after the final KA dose were selected for further

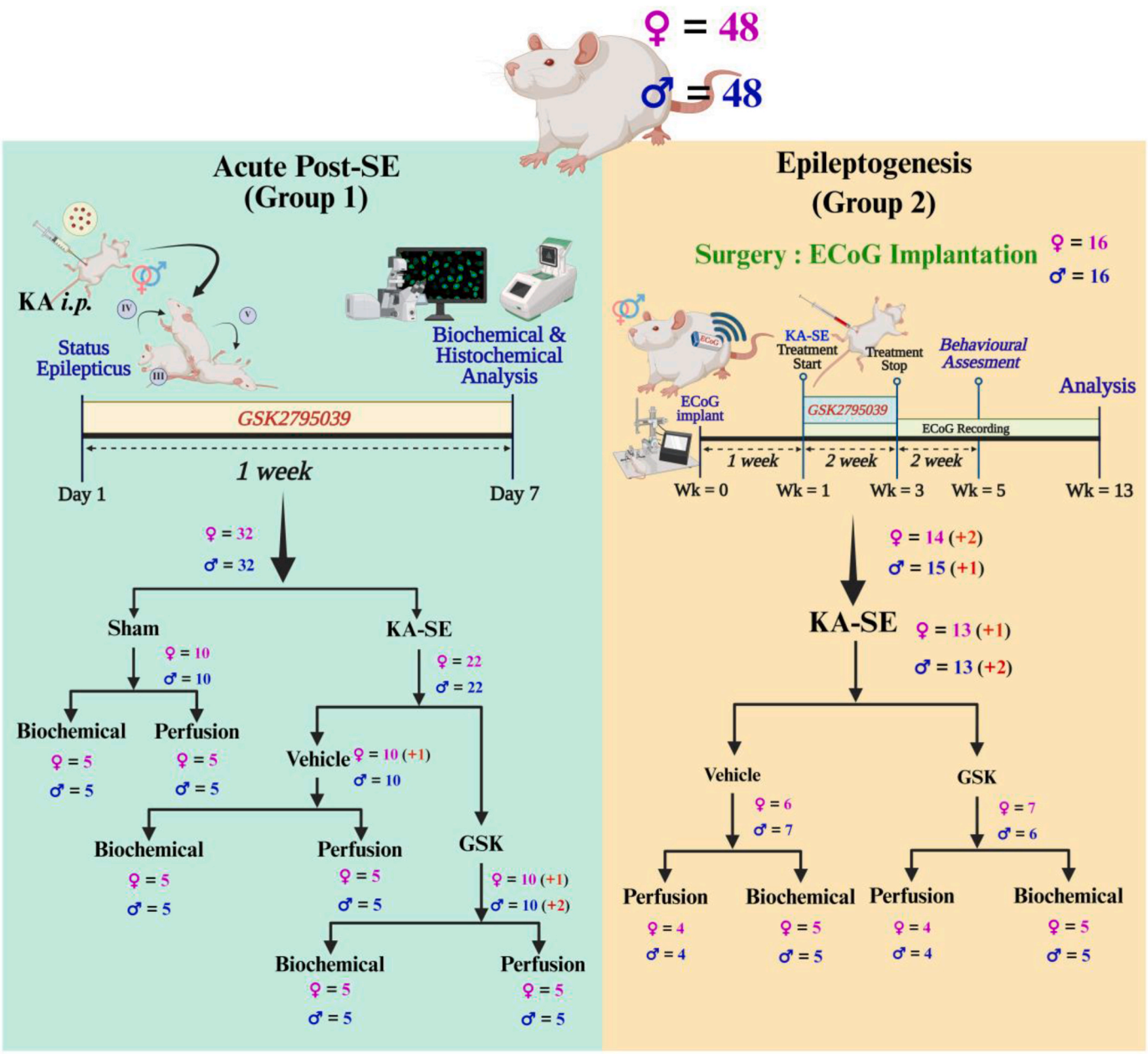

Fig. 1. Experimental design and animal grouping.
Schematic illustration experimental timeline for both acute post-SE group (Group 1) and epileptogenesis monitoring group (Group 2). Following timeline, animals were allocated (n = 96 animals; 48 male & 48 female rats) into both experimental groups. Group 1 (left, no surgery) consisted of animals that underwent KA-SE or sham treatment, received vehicle or GSK therapy for 1 week, and were sacrificed for biochemical and histological analysis (5-5 animal per group). Group 2 (right, surgery) animals underwent ECoG implantation followed by KA-SE induction and received vehicle or GSK therapy for 2 weeks. All survived animals were monitored for spontaneous seizure activity for 12 weeks to assess epilepsy progression and seizure burden. Red-highlighted numbers indicate animals that did not survive the experiment. Illustration was created in https://BioRender.com.

experimentation. SE induction in all ECoG-implanted animals from the vECoG monitoring group (detailed in the following section) was conducted under continuous ECoG monitoring to capture real-time ECoG activity during SE development.

2.1.4. Drugs administration

All animals were randomly assigned to either a two-group vehicle or treatment, as explained above. The pharmacological inhibitor of NOX2, GSK2795039 (GSK, Ambeed; dissolved in 10 %DMSO, 20 % Tween 80, 60 % PEG-200, 10 % Saline) was administered intraperitoneally 20 mg/kg/day for two weeks in the treatment group and equivalent volume of vehicle were administered intraperitoneally in vehicle group. For biochemical investigations, animals were treated with either GSK or Vehicle for 1 week following SE. For the antiepileptogenic ECoG monitoring experiment, animals were treated for two weeks either of GSK or Vehicle.

2.1.5. Video-electrocorticography: ECoG data acquisition and analysis

All subdural (ECoG) transmitter implanted animals, from anti-epileptogenic ECoG monitoring group, were housed individually subjected to 24/7 wireless vECoG monitoring. Wireless ECoG telemetry was controlled using Neuroarchiver software (Open-Source Instrument Inc.). Briefly, ECoG data were segmented into 4-s epochs, and six metrics were analyzed: power, intermittency, coastline, coherence, asymmetry, and

power within the 12–30 Hz range. Each metric was normalized to a 0–1 interval and compared to a user-generated seizure library, that included seizures from at least three different animals (https://www.opensourceinstruments.com/Electronics/A3018/Event_Detection.html). Epochs were classified as seizure like events if their Euclidean distance was less than 0.2 from a validated seizure epoch. All electrographic seizures were confirmed by visual inspection by a researcher blinded to treatment. Moreover, randomly selected seizures were further characterized through video monitoring using digital time-locked CCTV cameras (Microseven) positioned outside the cages, by research blinded to treatment.

2.1.6. Interictal spike analysis

ECoG data were analyzed using a random forest classifier and epochs were reviewed by two experts to manually classify them in baseline and spike activity. From each 1 s epoch, 17 features including statistical (skewness, kurtosis, 25 percentile, 10 percentile, variance, span, maximum, minimum, standard deviation, coastline) and frequency-domain parameters (absolute power, power in 1–100 Hz bands: 1–4 Hz, 4–8 Hz, 8–12 Hz, 12–30 Hz, and 30–100 Hz power), were extracted using standard Python libraries and clustered using t-distributed Stochastic Neighbor Embedding (t-SNE). The classifier was trained and tested using a stratified 70:30 split over 1000 iterations. Performance was assessed using a confusion matrix and F1 score analysis, with comparisons to shuffled test labels to ensure reliability. To test robustness, models were trained on data from one rat and tested on the others, with performance compared to randomly shuffled test samples.

2.2. Quantitative real-time polymerase chain reaction (qRT-PCR)

Total RNA from the cortex and hippocampus were extracted using Tri-Reagent (Sigma-Aldrich, St. Louis, MO, USA) and stored at − 80 °C following animal sacrifice. The purity and quantity of the extracted samples were confirmed using NanoDrop One^{C} (Thermo Scientific Inc., USA). Complementary DNA (cDNA) was synthesized using 1 μg of extracted RNA using oligo-dT15 primers and the GoScript™ Reverse Transcription System (Promega, Madison, WI, USA). Real Time PCR were carried with 15 μL of final reaction volume [7.5 μL of SYBER Green (PerfeCTa SYBR Green FastMix, Quantabio), 3 μL of primers mix (500 nM each), 1.5 μL of DEPC water (Thermo Scientific™), and 3 μL of cDNA template] using Real-Time PCR Detection System (CFX Connect, Bio-Rad, USA). The following cycling parameters were used: 10 min at 95 °C, followed by 40 cycles of denaturation at 95 °C for 5 s, and 60 °C for 15 s; and finally, 5 s at 65 °C, and 30 s at 95 °C. Primer sequences are reported in Table 1. Each RT-PCR reaction was conducted in duplicates. The level of target gene's mRNA were quantified relative to the housekeeping gene (GAPDH) using Pfaffl et al., 2001 method [27]. Results were expressed as Relative 'target gene' mRNA level, normalized to the sham operated animals.

2.3. Tissue collection and sample preparation

All animals were sacrificed at the end of experiment by deep anesthesia using intraperitoneal injection of Ketamidor (100 mg/kg; Richter Pharma AG) and Sedaxylan (10 mg/kg; Eurovet Animal Health B.V.), followed by transcardial perfusion with 1x PBS heparin, then 4 % paraformaldehyde (PFA) in PBS (Sigma). Brain samples were collected and stored overnight in 4 % PFA/PBS (37 %; Sisco Research Laboratories, SRL) at 4 °C, followed by cryoprotection using a gradient of sucrose 10-20-30 % for 3–4 days until the tissue sank. After cryoprotection, brain samples were immersed in OCT compound (Scigen) and stored at −80 °C. Sections were prepared using a cryostat (Leica CM1950) at −20 °C, with 25 μm thickness, and collected on poly-L-lysine coated slides (Thermo Fisher Scientific).

Table 1
List of primers used for RT-PCR.

Target Gene	Forward	Reverse
GAPDH	GACATGCCGCCTGGAGAAAC	AGCCCAGGATGCCCTTTAGT
IL-6	GACTTCCAGCCAGTTGCCTT	CTGGTCTGTTGTGGGTGGTAT
IL-1β	CCCTGCAGCTGGAGAGTGTGG	AGCACCTCTCAAGCAGAGCACA
IL-10	AATAAGCTCCAAGACAAAGGT	CTGCATAGAAGCCTACGTGA
TNFα	ATGGGCTCCCTCTCATCAGT	GCTTGGTGGTTTGCTACGA

2.4. Immunohistochemistry and microscopy

Brain sections containing slides were circled around the section using a water-repellent pen (Dako pen; Agilent) and washed with 1x PBS for 1 min. The sections were permeabilized with 0.2 % Triton X-100 (Sigma) in 1x PBS for 30 min, followed by blocking with 7 % goat serum (Vector Laboratories) in 0.1 % Triton X-100 in 1 % BSA (MP Biomedicals) in 1x PBS for 2 h. After blocking, sections were washed three times (10 min each wash) with 1x PBS. Sections were incubated overnight at 4 °C with a primary antibody mixture: *Anti*-NeuN (rabbit, 1:500, ab177487) for neurons; Anti-8OH'dG (mouse, 1:500, ab62623) for DNA damage, prepared in 0.1 % Triton X-100 in 1 % BSA in 1x PBS. Following overnight incubation, sections were washed (as described above) in 1x PBS and then incubated for 2 h in the dark in a secondary antibody's mixture: Alexa Fluor®-488 goat anti-rabbit (1:500, ab150081); Alexa Fluor®-568 goat anti-mouse (1:500, ab175701). Following incubation, the sections were washed (as described above) in 1x PBS and allowed to dry and mounted with 4′,6-diamidino-2-phenylindole (DAPI) mounting medium (Abcam).

All Immunohistochemical Images were captured using a Nikon Confocal A1R microscope with 10x objectives. To ensure signal specificity and minimize background fluorescence, standard negative controls, such as sections processed without primary antibodies were included during protocol optimization. Imaging settings were kept constant across all samples to ensure consistency and comparability. Image analysis was performed using NIS Elements Advanced Research Software. The mean intensity was calculated and normalized to the average of the sham-operated animals. Results are expressed as Mean Fluorescence Intensity (A.U.), (Normalized to Sham).

2.5. Nissl staining and imaging

Neuronal death in the hippocampus was assessed by Nissl staining. Coronal brain sections (25 μm thick) were first dried and placed directly into 1:1 alcohol/chloroform overnight and then rehydrated through a graded alcohol series (100 %, 95 %, and distilled water, each for 5 min). The sections were subsequently stained with 0.1 % cresyl violet (Thermo Scientific, USA) for 5–10 min and rinsed with distilled water. Differentiation was performed in 95 % alcohol for 15–30 min, followed by dehydration in absolute alcohol twice for 5 min each. The sections were then cleared in xylene twice for 5 min each and mounted using Eukitt® Quick-Hardening Mounting Medium (Sigma-Aldrich, USA).

Bright-field images were acquired with a SideView VS200 digital slide scanner (VS200 Multiple Tray Loader, Olympus) using a 20x objective under bright-field illumination, controlled via Olympus VS200 software. Image analysis was performed manually to quantify Nissl-stained neurons in the CA1 and CA3 subfields of the hippocampus under different experimental conditions. Results were expressed as neuronal density per mm^2 normalized to sham in both subfields.

2.6. Behavioral assessment

All ECoG implanted animals from the antiepileptogenic ECoG monitoring experimental group were subjected to behavioral assessment at two weeks after completing the SE and two weeks of vehicle or GSK therapy. Novel Object Recognition (NOR) and T-maze alternation tests were performed to assess the effects of GSK therapy on cognitive

behaviors such as spatial learning and recognition memory. Elevated Plus Maze (EPM) and Open Field (OF) tests were performed to assess the anxiety like behaviors.

2.6.1. Elevated Plus Maze (EPM)

The EPM consists of two opposing open arms (50 × 12 cm) and two enclosed arms (50 × 12 cm) extending from a central platform (12 × 12 cm), elevating 50 cm above the floor. The day before the test, each animal was placed in the center of the maze and allowed to explore for approximately 10 min. On the test day, the animals were positioned at the intersection of the open and closed arms to start a 10-min test. During the test, the animal may spend time in either the closed (safe) or open arms. All movements were recorded using an overhead CCTV camera, and footage was analyzed for total no. of entries and percentage of time spent in open arms using a semi-automatic script of DeepLabCut™ (https://github.com/DeepLabCut) [28]. The maze was cleaned with 70 % ethanol between each animal.

2.6.2. Open Field (OF)

The OF maze consisted of a plexiglass box measuring 100 × 100 × 40 cm. The animals were placed in the arena and allowed to move freely for 10 min while being recorded using an overhead CCTV camera. The CCTV footage was analyzed using EthoVision XT software. During the 10-min test period, the total distance moved by the animal and the percentage time spent in the center of the arena (50 × 50 cm) were tracked and measured. The maze was cleaned (as described above) between each experiment.

2.6.3. Novel Object Recognition (NOR)

The NOR test was conducted in the same OF arena measuring 100 × 100 × 40 cm. During the familiarization phase, each animal was placed in the arena containing two identical objects and allowed to explore for a predetermined period of 10 min. After a delay of 90 min, one of the familiar objects was replaced with a novel object. The animals were then reintroduced into the arena for a test session of the same duration. The time spent exploring each object during both the familiarization and test phases was recorded by using an overhead CCTV camera. Recognition memory was assessed by comparing the exploration time of the novel object during the test session with that of the familiar object, with increased exploration of the novel object indicating successful recognition. To minimize olfactory cues, the arena and objects were cleaned with 70 % ethanol between trials. The order of object presentation was counterbalanced to control for side bias.

2.6.4. Spontaneous alternation T-maze

The T-maze used in this study consisted of a symmetrical T-shaped structure with a central stem and two perpendicular arms (50 × 12 cm). In each trial, the animals were placed in the start box and allowed to navigate through the stem, where they could choose either arm. To be considered as entering a specific arm, the animals must enter it with all four limbs. Once the animal entered the goal arm, the guillotine door was closed for 30 s, after which the animal was returned to the starting box for the next trial. The intertrial interval was 1 min. For each trial, the arms selected by the animals were recorded using an overheaded CCTV. After six trials, the total number of alternations was calculated and the percentage bias for each rat was measured using the following formula: (total number of correct alternations/6) × 100. All experiments were conducted by an experimenter blinded to the treatment group.

2.7. Statistical analysis

Statistical analyses were conducted using GraphPad Prism v9.3.1 (GraphPad Software, USA). Data acquisition and analysis were performed by a researcher blinded to treatment. All quantitative results are presented as the mean ± standard error of the mean (s.e.m.), with n representing the number of individual samples. Data were analyzed using unpaired Student's t-test, one-way analysis of variance (ANOVA) with Tukey's post hoc test, or two-way ANOVA with Tukey's or Dunnett's post hoc test, as appropriate for the experimental design. Seizure frequency was analyzed using a generalized log-linear mixed model, incorporating the random effect of the animal (autoregressive covariance) and fixed effects of treatment group, week, and their interaction. Statistical significance was set at $p < 0.05$. Sample sizes were determined based on prior experience in assessing experimental variability. The number of animals used in each experiment is indicated in the corresponding figure legends.

3. Results

3.1. Selective NOX2 inhibition by GSK2795039 attenuates SE-induced neuroinflammatory responses

Status epilepticus is known to trigger a robust neuroinflammatory cascade characterized by the upregulation of pro-inflammatory cytokines [29–34] and oxidative stress [35–37], which contributes to the progression of epileptogenesis [12,38–40]. NOX2, a major source of ROS in the brain, rapidly upregulated following SE and its activation has been closely linked to the induction and amplification of neuroinflammation [7,8,40–43]. Previous studies have demonstrated that SE induces the expression of proinflammatory cytokines such as interleukin-6 (IL-6), interleukin-1β (IL-1β), and tumor necrosis factor-α (TNFα), which mediate neuronal damage and glial activation [10,29,44–47]. Wu et al. (2015) showed that genetic deletion of NOX2 subunits in mice significantly attenuates SE-induced upregulation of these cytokines, highlighting the pivotal role of NOX2-derived ROS in mediating neuroinflammatory cascades [44]. Based on previous evidence, we hypothesized that immediate pharmacological inhibition of NOX2 using GSK2795039, a selective and functional NOX2 inhibitor, could exert secondary inhibitory effects on the expression of inflammatory cytokines following SE.

To test this, we employed a well-validated kainic acid induced status epilepticus model for temporal lobe epilepsy [48,49]. In our experimental design (Fig. 1; Group 1), animals under acute post SE group underwent SE induction via KA and were subsequently treated with either vehicle or GSK2795039 for seven days to assess the effect of NOX2 inhibition on SE induced inflammatory responses. This treatment window was selected to target the early phase of epileptogenesis following initial insult of SE, during which neuroinflammatory and oxidative process are most dynamic [10,50,51]. We assessed the expression of pro-inflammatory (IL-6, IL-1β, and TNFα) and anti-inflammatory (IL-10) cytokines in the hippocampus (Fig. 2A–H) and the cortex (Fig. 2I–P) of male and female animals. Following SE, proinflammatory cytokines expression increased robustly in the hippocampus of vehicle treated animals, IL-6 ($F(2,27) = 49.28$, $p < 0.0001$, Fig. 2A); IL-1β ($F(2, 27) = 58.34$, $p < 0.0001$, Fig. 2B); and TNFα ($F(2, 27) = 45.09$, $p < 0.0001$, Fig. 2C), which was significantly reduced by GSK treatment: IL-6 ($p < 0.0001$ vs SE + Veh, Fig. 2A), IL-1β ($p < 0.0001$ vs SE + Veh, Fig. 2B), and TNFα ($p < 0.0001$ vs SE + Veh, Fig. 2C). The level of IL-10 showed no significant change in the vehicle-treated group ($p = 0.689$, Fig. 2D), but the levels following GSK treatment were significantly increased compared to the vehicle ($p < 0.001$, Fig. 2D). The GSK treatment-induced anti-inflammatory response prompted further investigation, confirming potential sex-dependent differences in expression and drug response. A two-way ANOVA was performed to assess the effects of sex and treatment. Interestingly, pro-inflammatory cytokines exhibited only sex-dependent differential expression, IL-6 ($F(2, 24) = 46.78$, $p < 0.0001$, Fig. 2E), IL-1β ($F(2, 24) = 56.86$, $p < 0.0001$, Fig. 2F), and TNFα ($F(2, 24) = 44.11$, $p < 0.0001$, Fig. 2G). For IL-10, both main effects of sex ($F(2, 24) = 16.71$, $p < 0.0001$) and treatment ($F(1, 24) = 11.51$, $p = 0.0024$), as well as the interaction between sex and treatment ($F(2, 24) = 3.556$, $p = 0.0444$), were found to be statistically significant.

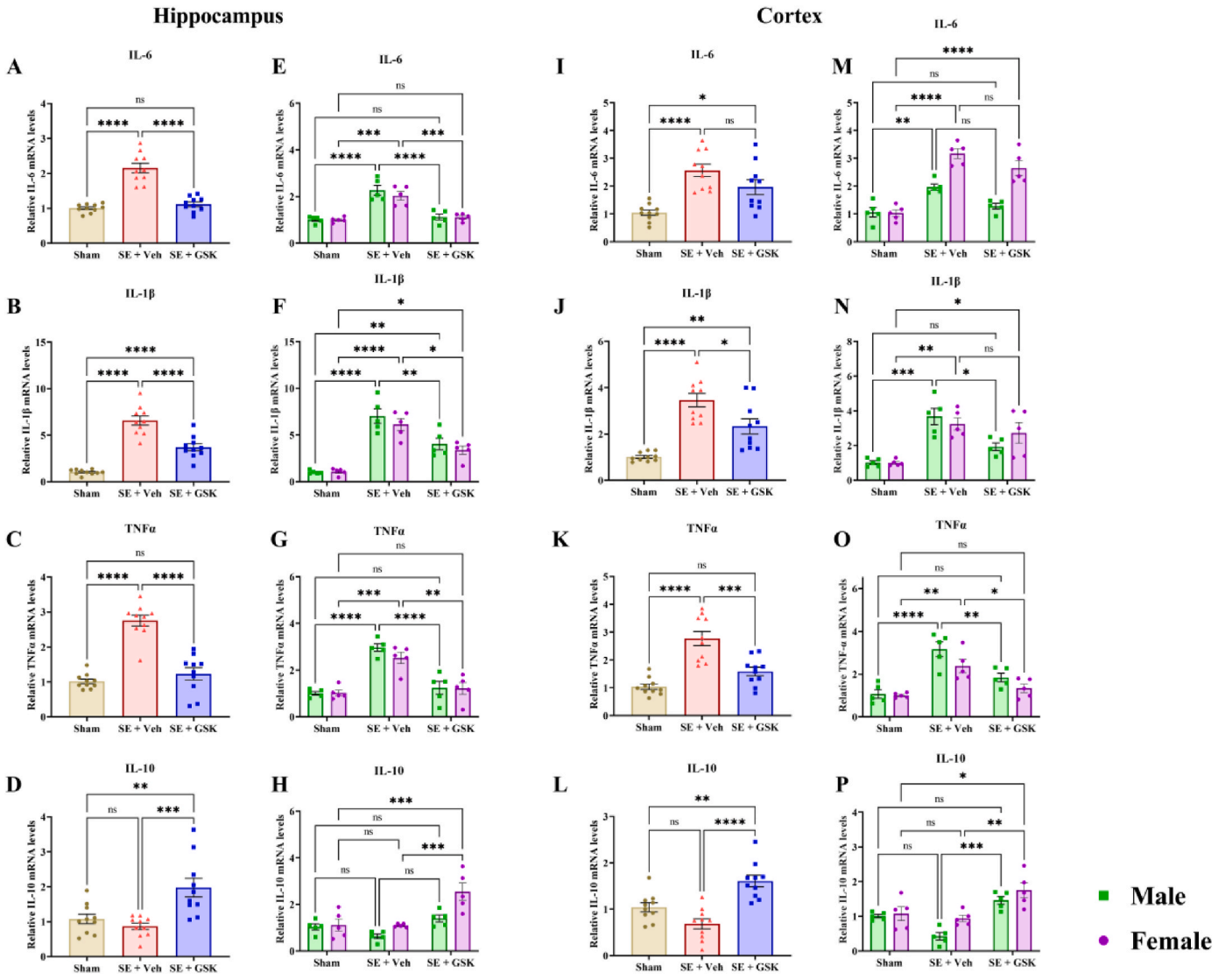

Fig. 2. Selective NOX2 inhibition by GSK2795039 modulates SE-induced inflammatory cytokines.
(A–D) Male and female combined relative mRNA expression of proinflammatory cytokines IL-6 (A), IL-1β (B), and TNFα (C) and anti-inflammatory cytokines IL-10 (D) in hippocampus following one week of vehicle or GSK treatment after SE. (E–H) Relative mRNA expression, male (green) vs female (purple), of pro-inflammatory cytokines IL-6 (E), IL-1β (F), and TNFα (G) and anti-inflammatory cytokines IL-10 (H). (I–L) Male and female combined relative mRNA expression of proinflammatory cytokines IL-6 (I), IL-1β (J), and TNFα (K) and anti-inflammatory cytokines IL-10 (L) in cortex following one week of vehicle or GSK treatment after SE. (M – P) Relative mRNA expression of pro-inflammatory cytokines IL-6 (M), IL-1β (N), and TNFα (O) and anti-inflammatory cytokines IL-10 (P). n = 5 animals per sex per group. Data are presented as mean ± s.e.m. Statistical significance was determined either by one-way ANOVA (A-D, and I-L), where males and females were combined, or by two-way ANOVA (E-H, and M – P) with Sex and Treatment as factors, followed by Tukey's post hoc test for multiple comparisons. *$p < 0.05$, **$p < 0.01$, ***$p < 0.001$, ****$p < 0.0001$, ns: not significant.

In cortex, we observed similar trend of induction of proinflammatory cytokines expression: IL-6 ($F(2, 27) = 13.71$, $p < 0.0001$, Fig. 2I); IL-1β ($F(2, 27) = 23.44$, $p < 0.0001$, Fig. 2J); and TNFα ($F(2, 27) = 23.84$, $p < 0.0001$, Fig. 2K), in vehicle treated animals but unlike in the hippocampus, GSK fail to inhibit IL-6 ($p = 0.118$ vs. SE + Veh Fig. 2I), but inhibited IL-1β ($p = 0.010$ vs SE + Veh, Fig. 2J), and TNFα ($p = 0.0002$ vs SE + Veh, Fig. 2K). Similar to the hippocampus, the expression of the anti-inflammatory cytokine IL-10 was not significantly changed ($p = 0.0730$ vs. SE + Veh, Fig. 2L) in the vehicle-treated group, but this rescued the elevated levels following GSK treatment ($p < 0.0001$, Fig. 2L). Consistent with the hippocampus, the cortex exhibited sex-dependent difference in expression of IL-6: ($F(2, 24) = 43.01$, $p < 0.0001$, Fig. 2M), IL-1β: ($F(2, 24) = 23.69$, $p < 0.0001$, Fig. 2N), TNFα (($F(2, 24) = 28.09$, $p < 0.0001$, Fig. 2O), and IL-10 ($F(2, 24) = 21.7$, $p < 0.0001$, Fig. 2P). Interestingly, IL-10 expression was rescued to a greater extent following GSK treatment in male animals' cortex and hippocampus (Fig. 2H–P, respectively), while in female cortex only (Fig. 2H–P, respectively) compared to vehicle treated group.

Altogether, these findings confirmed that GSK inhibited the SE-induced pro-inflammatory response and rescued the anti-inflammatory cytokines in hippocampus with possibility of sex-dependent responses to SE and GSK therapy.

3.2. *Effect of GSK treatment on SE-induced oxidative DNA damage in hippocampal neurons*

Oxidative stress is a well established consequence of SE, leading to neuronal injury through mechanisms such as DNA and RNA damage [52–55]. Among markers of oxidative damage to DNA, 8-hydroxy-2′-deoxyguanosine (8-OHdG) is widely used for its sensitivity and specificity in detecting oxidative modifications [56] in both preclinical and clinical studies [57–61]. The hippocampus is especially susceptible

to seizure induced oxidative injury due to its high metabolic demand and dense neuronal population, making it a key region for evaluating neuroprotective strategies. Notably, oxidative DNA damage is a critical factor in epileptogenesis, as persistent DNA lesions can disrupt neuronal homeostasis, activate cell death pathways, and promote neuroinflammation [62–64].

Next, we specifically examined whether GSK mitigates SE induced oxidative DNA damage in hippocampal neurons of both male and female animals. By assessing 8-OHdG (marker of DNA oxidation) immunoreactivity co-localized with NeuN-positive neurons, we demonstrated oxidative DNA damage in the hippocampus of male (Fig. 3A–D) and female (Fig. 3E–H) animals. GSK significantly mitigated SE-induced oxidative DNA damage (mean fluorescence intensity reflecting the relative proportion of DNA damage) in both CA1 (Fig. 3A–C) and CA3 (Fig. 3B–D) subfields of hippocampus compared to vehicle treated group in male animals. In female animals, SE induction resulted in a reduction of 8-OHdG intensity in the CA1 region of the vehicle group, while GSK treatment did not produce a significant change in this marker (Fig. 3E–G), suggesting the possibility that the pattern of oxidative DNA damage following SE may differ between sexes, potentially reflecting sex specific susceptibility to neuronal injury (Fig. 3E) or the activation of alternative cell death pathways in females. Despite the lack of significant changes in mean fluorescence intensity in the CA3 region across conditions (Fig. 3F–H), neuronal loss was still evident in both CA1 and CA3 subfields (Fig. 3E and F). These findings indicate that 8-OHdG may not fully capture the complexity of oxidative damage in female hippocampal neurons after SE, and that other forms of oxidative injury or compensatory mechanisms could be involved.

3.3. Protective effect of GSK treatment on SE-induced neuronal death

Following the demonstrated efficacy of GSK in mitigating SE induced oxidative DNA damage in hippocampal neurons, we next sought to determine whether this protection also translates into preservation of neuronal integrity. Oxidative DNA damage is closely associated with neuronal loss after SE, particularly in the vulnerable CA1 and CA3 subfields of the hippocampus [62,65–67]. Therefore, we assessed the extent of neuronal death in these regions to further evaluate the

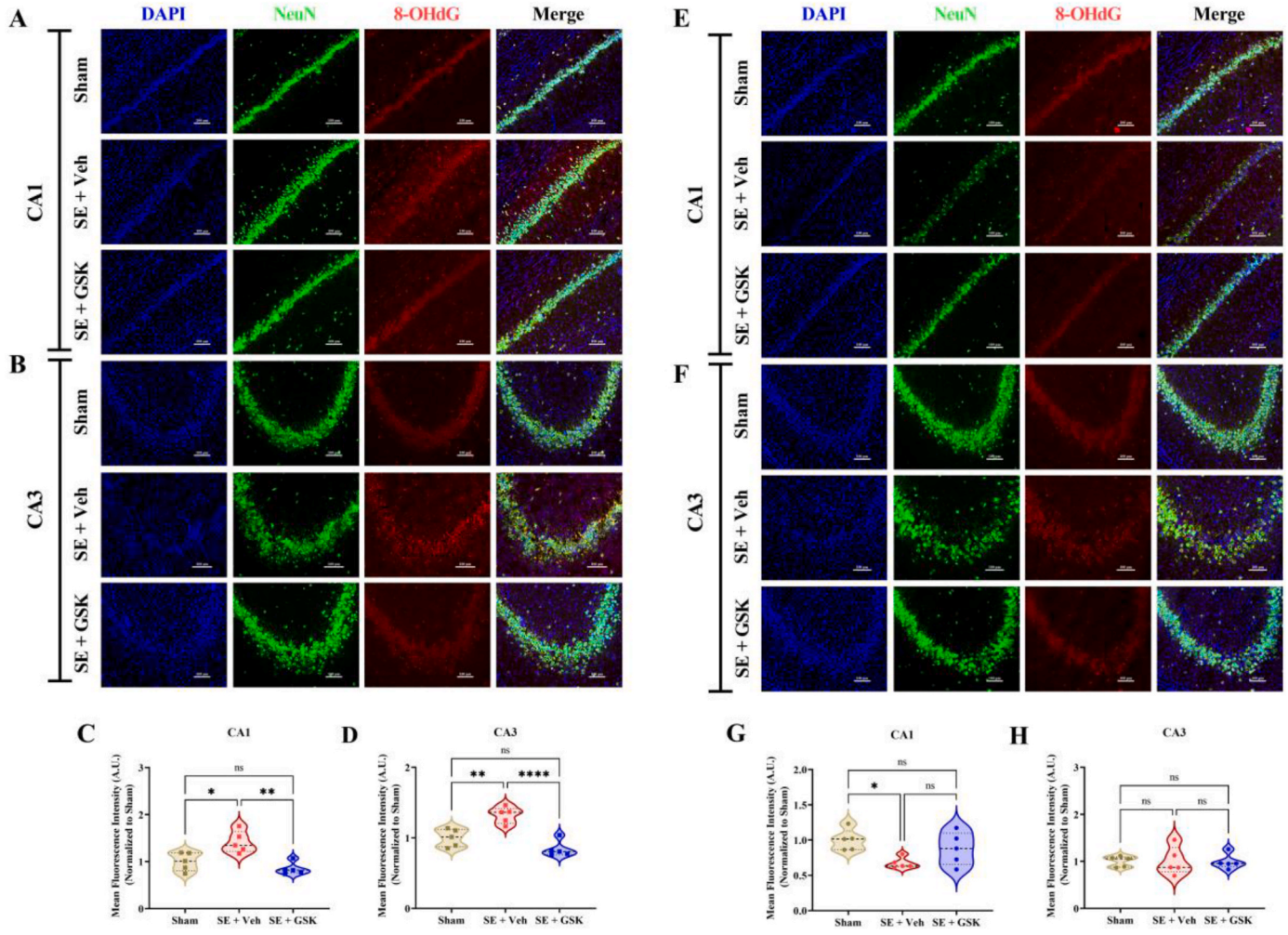

Fig. 3. GSK treatment reduces SE-induced oxidative DNA damage in hippocampal neurons of male animals.
Representative immunofluorescence images of the CA1 (A) and CA3 (B) subregions of the hippocampus from sham, vehicle, and GSK-treated male rats post-SE. Hippocampal subfields were anatomically identified using standard references and outlined using DAPI nuclear staining (blue). Sections were stained with DAPI (blue), NeuN (green, neuronal marker), and 8-OHdG (red, marker for oxidative DNA damage). Co-localization of 8-OHdG with NeuN shows oxidative DNA damage in neurons. (C, D) Quantification of 8-OHdG means fluorescence intensity (arb. unit) in the CA1 (C) and CA3 (D) subfields of the hippocampus. Representative immunofluorescence images of the CA1 (E) and CA3 (F) subfields of the hippocampus from sham, vehicle- or GSK-treated SE female animals. (G, H) Quantification of 8-OHdG means fluorescence intensity (arb. unit) in the CA1 (G) and CA3 (H) subfields of the hippocampus. n = 5 animals per group. Data are expressed as mean ± s.e.m. Statistical significance was determined by one-way ANOVA followed by Tukey's post hoc test. *p < 0.05, **p < 0.01, ****p < 0.0001, ns: not significant. Scale bars, 100 μm.

neuroprotective potential of GSK treatment.

We observed a significant reduction in neuronal density in the CA1 and CA3 subfields of the hippocampus in both male (Fig. 4B and C, respectively) and female animals (Fig. 4E and F, respectively) one week after SE in vehicle-treated groups compared to sham, indicating SE-associated neuronal death in both subfields. Notably, GSK therapy prevented this SE associated neuronal death in both CA1 and CA3 subfields in the hippocampus of male (Fig. 4B and C) and female (Fig. 4E and F) GSK treated animals. However, SE-associated loss of neuronal integrity in females appeared more severe, with distorted and shrunken neuronal populations in both CA1 and CA3 (Fig. 4D) subfields of vehicle treated animals. This damage was only partially prevented by GSK treatment, suggesting the possibility of limited NOX2 involvement in females following SE mediated neuronal death.

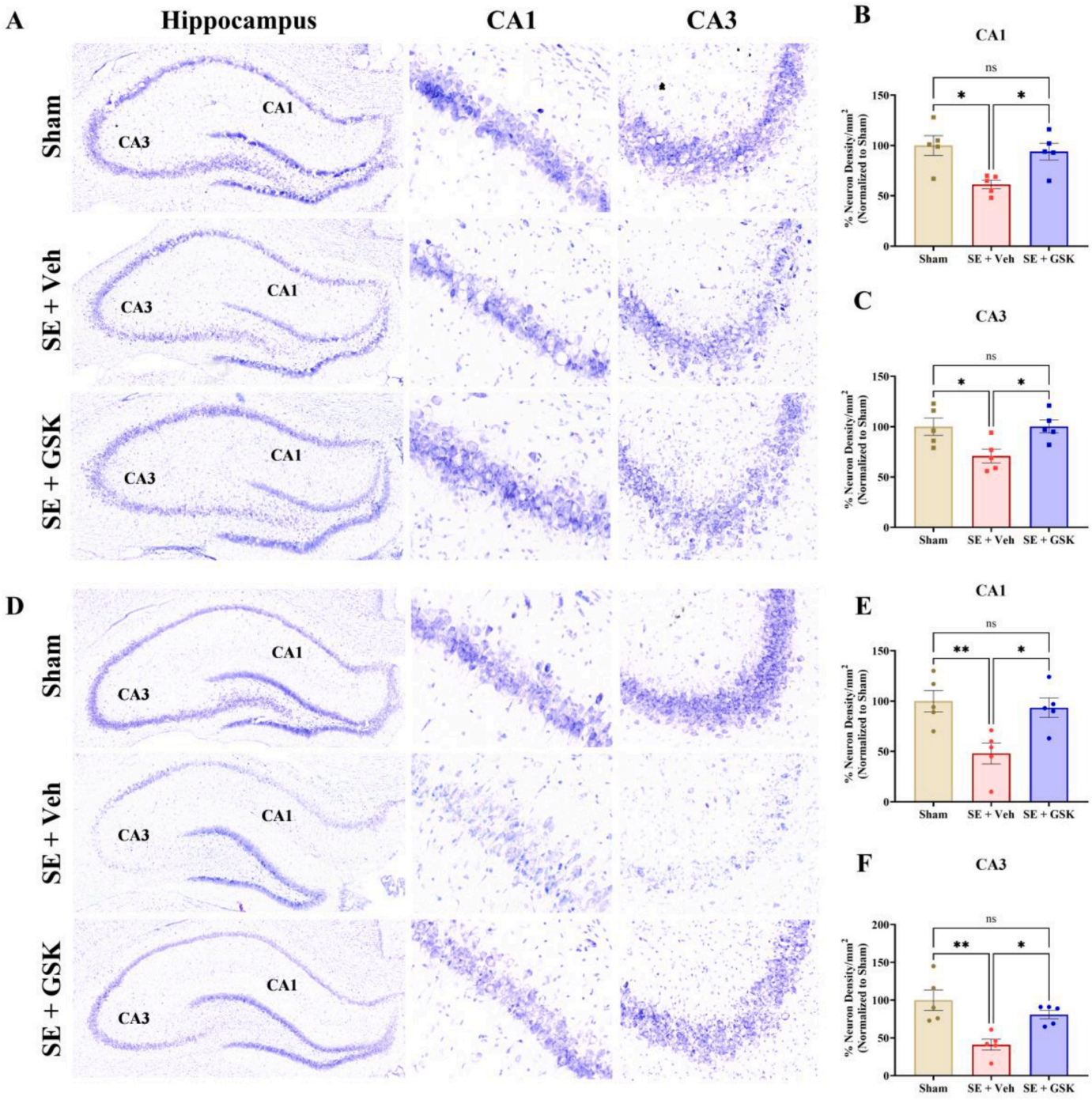

Fig. 4. GSK exert neuroprotective effect against SE induced neuronal death in hippocampus.
Representative Nissl-stained coronal sections of the hippocampal CA1 and CA3 subfields, identified using standard anatomical landmarks, are shown for male (A) and female (D) rats from sham, vehicle- and GSK-treated groups following SE. Middle and right panels show higher magnification views highlighting neuronal density and structural integrity. Quantification of neuronal density in the CA1 (B, E) and CA3 (C, F) regions is presented for male (B–C) and female (E–F) animals, respectively. n = 5 animals per group. Data are expressed as mean ± s.e.m. Statistical significance was determined by one-way ANOVA followed by Tukey's post hoc test. *$p < 0.05$, **$p < 0.01$, ns: not significant.

3.4. GSK therapy mitigates the development of epilepsy following KA-induced SE

We further assessed the long-term effect of NOX2 inhibition with GSK on epilepsy development and progression and investigated possible sex-dependent therapy responses. We induced SE and randomly assigned male and female animals (for which we did not observe any difference in any of the quantified parameters, Supp Fig. 1) into vehicle and GSK therapy groups (Fig. 1; Group 2). SE induction was performed with ECoG monitoring, and the duration of SE was recorded. The SE duration ranged from 125 to 182 min (163 ± 4 min) in the vehicle group, and from 147 to 205 min (170 ± 5 min) in the GSK group (Supp Fig. 1). After SE, all allocated animals underwent daily GSK or vehicle injections for two weeks, and the vECoG monitoring continued up to 12 weeks (Fig. 5A).

The absolute number of seizures per week analysis revealed a progressive increase in seizure frequency and in general higher seizure burden following SE in vehicle-treated animals over time (Fig. 5A–B), in comparison to GSK treated animals which experienced significantly lower seizure frequency and burden throughout the 12 weeks of vECoG

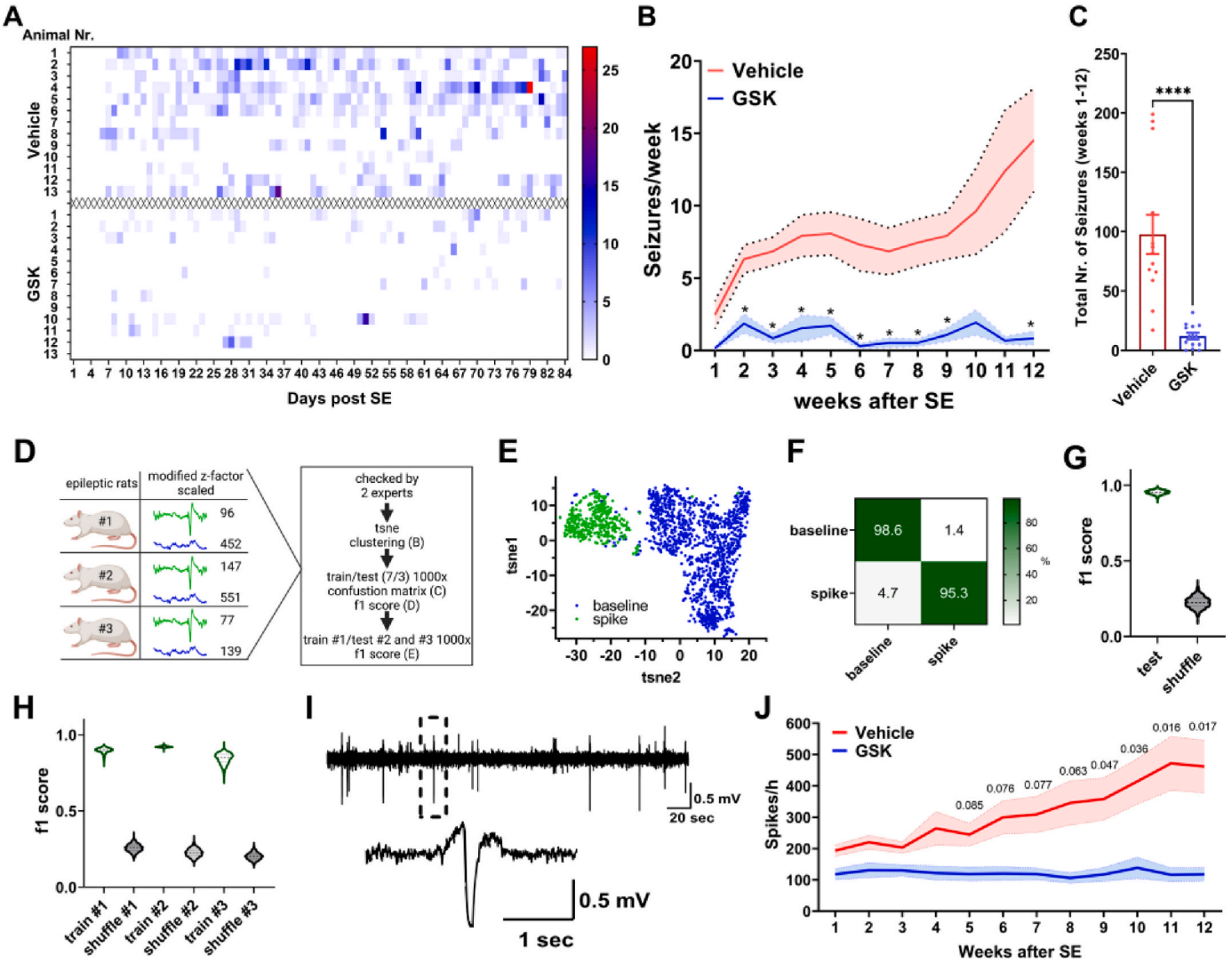

Fig. 5. GSK therapy reduces seizure burden, interictal spikes, and suppresses the development of epilepsy following SE.
(A) Raster plot showing seizure frequency in the vehicle-treated (top) and GSK-treated (bottom) animals over 12 weeks following SE, including initial two weeks of the treatment window after SE. Seizure numbers are color-coded by frequency, with higher seizure counts indicated by warmer colors (white to blue to red). (B) Weekly seizure frequency in vehicle (red) and GSK (blue) treated animals. (C) Total number of seizures experienced by animals in B. (D–H) Machine learning approach for detecting interictal spikes. (D) Schematic representation of dataset used to develop the random forest classifier. In total 1462 1 s modified z-score scaled (scaled to a 1 h ECoG signal) fragments from three different rats were analyzed by two experts and manually classified as baseline or spike activity. (E) t-SNE clustering of extracted features (17 features per 1 s epoch, as detailed in the Methods) demonstrates the model's ability to distinguish between baseline (blue) and spike (green) activity. (F) The confusion matrix showing the classifier's accuracy in differentiating baseline from spike activity. (G) F1 score evaluation showing high classification reliability, with the test dataset achieving a near-perfect F1 score, while randomly shuffled test data show significantly lower scores. (H) Robustness test of the classifier across different rats: random forest classifiers were trained on one rat [rat#1 (train #1), rat#2 (train #2), or rat#3 (train #3)] and tested on the remaining two. The model maintained a high F1 score, confirming its robustness even when trained on separate datasets. Randomly shuffled test data serve as a control. (I) Representative ECoG trace illustrating frequent interictal discharges; the inset shows a magnified view of a single spike. (J) Quantification of cumulative spike frequency per hour, in vehicle-treated (red) and GSK-treated (blue) animals over 12 weeks following SE. n = 13 animals (A–C). Data are presented as mean ± s.e.m. Statistical significance, of seizure frequency (B) was analyzed using a generalized log-linear mixed model, incorporating the random effect of the animal (autoregressive covariance) and fixed effects of treatment group, week, and their interaction, by unpaired *t*-test (C), or repeated-measures two-way ANOVA (J). *p < 0.05, **p < 0.01, ****p < 0.0001, ns: not significant.

monitoring duration (Fig. 5A–B). The cumulative number of seizures experienced by each animal over 1–12 weeks confirmed that GSK-treated animals experienced significantly fewer seizures compared to vehicle group (Fig. 5C, $p < 0.0001$, unpaired *t*-test), suggesting that early NOX2 inhibition exerts sustained seizure suppressive effects.

ECoG monitoring confirmed the absence of sex dependent differences in the duration of SE induction (Supp Fig. 1B–D). However, sex specific analysis of treatment response revealed a progressive increase in spontaneous recurrent seizure activity in vehicle-treated males compared to females, emerging from week 8 onward (Supp Fig. 2). While GSK therapy significantly reduced seizure frequency in both sexes, the extent of seizure suppression was greater in males (Supp Fig. 3A and C). Quantification of the total seizures over 12 weeks confirmed that male vehicle treated animals experienced a higher cumulative seizure burden than females (Supp Fig. 3B and D; 91 ± 20 vs. 47 ± 13 seizures, $p = 0.095$, unpaired *t*-test). GSK treatment resulted in a significant reduction in total seizures in both males (Supp Fig. 3B, $p < 0.01$, unpaired *t*-test) and females (Supp Fig. 3D, $p < 0.05$, unpaired *t*-test), however, the extent of seizure suppression was more pronounced in males than females (Supp Fig. 3). These findings indicate that NOX2 inhibition with GSK exerts long-lasting protective effects against epilepsy development following SE, with greater efficacy in males. The sex dependent differences in seizure suppression suggest that neuroinflammatory or oxidative stress mechanisms may differentially contribute to epileptogenesis in male and female animals.

3.5. GSK therapy suppresses interictal spiking and network hyperexcitability

To assess whether the effects of GSK therapy extend beyond seizure suppression, we investigated its effect on persistent interictal hyperexcitability. While seizure frequency measures overt epileptic events, interictal spikes serve as a marker of abnormal neuronal excitability and cortical dysfunction independent of seizures [68,69]. By analyzing interictal spike frequency, we aimed to determine whether NOX2 inhibition reduces prolonged network hyperactivity following SE, thereby mitigating a key contributor to epileptogenesis.

Interictal spiking frequency were analyzed using machine learning approach (Fig. 5D–H), showed the applied model has clear distinction ability between baseline and spike activity (Fig. 5E) with high classification accuracy (98.6 % for baseline, 95.3 % for spikes activity, Fig. 5F), without random classification (Fig. 5G–H). Quantification of cumulative interictal spike frequency across 12 weeks reveals a progressive increase in spikes per hr in vehicle-treated animals, whereas GSK treated animals maintained their significantly reduced interictal spike frequency throughout the 12 weeks of monitoring (Fig. 5J). Sex stratified analysis revealed distinct treatment responses to GSK, with marked differences observed between males and females (Supp Fig. 4A–B, respectively). In males, the vehicle-treated group demonstrated a progressive increase in interictal spike frequency, reaching over 600 spikes/hr by week 12 (Supp Fig. 4A). In contrast, GSK treated males exhibited a significantly reduced interictal spike rate across the 12 week period, with a maximum average value of only 191 spikes/hr ($p < 0.01$, Supp Fig. 4A). In females, vehicle treated animals exhibited an increase in interictal spike frequency over time, but to a lesser extent than in males (Supp Fig. 4B). GSK treated females exhibited a moderate yet statistically significant reduction in interictal spiking activity compared with the vehicle ($p < 0.05$, Supp Fig. 4B).

These findings indicate that NOX2 inhibition with GSK, mitigates interictal hyperexcitability in a sex-dependent manner, with greater efficacy in males. The suppression of interictal discharges suggests that oxidative stress modulation may play a critical role in limiting aberrant neuronal activity during epileptogenesis.

3.6. GSK therapy protects from cognitive deficits associated with epileptogenesis

Cognitive impairment, including deficits in learning, memory, and exploratory behavior, is a common and debilitating consequence of epileptogenesis and chronic epilepsy [70–72]. Oxidative stress and neuronal loss in the hippocampus are key contributors to these cognitive deficits [73,74]. Following the demonstrated neuroprotective and anti-epileptogenic efficacy of targeting NOX2 using GSK, we next evaluated whether early intervention with GSK after SE could also ameliorate cognitive decline associated with epileptogenesis.

In the open field test, male vehicle treated animals exhibited a less exploratory locomotor pattern with reduced time spent in the central area (Fig. 6A and B), whereas GSK treated males showed significantly increased locomotion and increased time spent in the central area for exploration (Fig. 6A and B), suggesting that GSK treated animals experienced less anxiety like behavior. A significant reduction in the total distance traveled, velocity, and over all movement duration (Supp Fig. 5A–C) in vehicle compared to GSK treated males further supports that GSK therapy rescued the reduced locomotor activity associated with epilepsy development. To investigate if the increased % center time is due to GSK induced behavioral arrest in the GSK treated group, we compared the automatic analyzed freezing time, for which we did not find a significant difference between vehicle and GSK treated animals (Supp Fig. 5D), which further supports our findings that elevated central area exploration time is not the result of coincidental behavioral arrest in GSK treated males leading to an increase in the central exploration time (Fig. 6B). Interestingly, females from the vehicle-treated group possessed higher locomotor activity (48.91 ± 7.92 m, Supp Fig. 5E; 8.16 ± 1.32 cm/s, Supp Fig. 5F) than vehicle-treated males (11.92 ± 2.39 m, Supp Fig. 5A; 2.33 ± 0.48 cm/s, Supp Fig. 5B) with extensive movement across the arena (Fig. 6A–C), and GSK treatment increased the central exploration time (Fig. 6D). In contrast to males, we observed no significant differences in total distance traveled, velocity, and overall movement duration (Supp Fig. 5E–G) between vehicle and GSK treated females. This suggests that GSK therapy may not have a measurable impact on locomotor activity in females under the tested conditions. We further validated the effect of GSK therapy on anxiety like behavior through elevated plus maze test. Male GSK-treated animals spent in open arms significantly more time than vehicle-treated males (Fig. 6E). Even though entries to the open arm by male-treated animals exhibited no significant difference across the experimental group (Supp Fig. 5I). Similar to males, female GSK-treated animals spent more time in the open arms than vehicle-treated females (Fig. 6F). In contrast, GSK-treated females exhibited significantly higher number of entries into the open arms (Supp Fig. 5J), suggested a less anxious phenotype in the GSK treated females. We further assessed the effect of GSK therapy on recognition, memory, and cognitive impairment in epilepsy using Novel Object Recognition (NOR) test. In this test, we observed the declined discrimination index (ranged from -0.79 to $+0.17$, Fig. 6G) in vehicle treated male animals suggesting their poor recognition memory and cognitive impairments. However, GSK therapy prevents associated declines in discrimination index (ranged from $+0.15$ to $+0.71$, Fig. 6G) suggesting the protective effect on GSK-treated male animals on their cognitive function and recognition memory compared male vehicle treated animals (Fig. 6G). Additionally, we also observed the increased exploration frequency for novel objects in GSK-treated males (Supp Fig. 5K). However, similar to males we observed declined discrimination index (ranged from -1.0 to $+0.38$, Fig. 6H) in vehicle treated female which were prevented in GSK treated females (DI, $+0.05$ to $+1.0$, Fig. 6H), while no significant changes were observed in exploration frequency for novel objects (Supp Fig. 5L). Finally, we evaluated the overall therapeutic outcome of GSK by demonstrating the effect of GSK on impaired working Memory and spatial learning through spontaneous T-Maze alteration test. We observed a declined rate of successful alteration in both male and female vehicle treated animals (Fig. 6I–J,

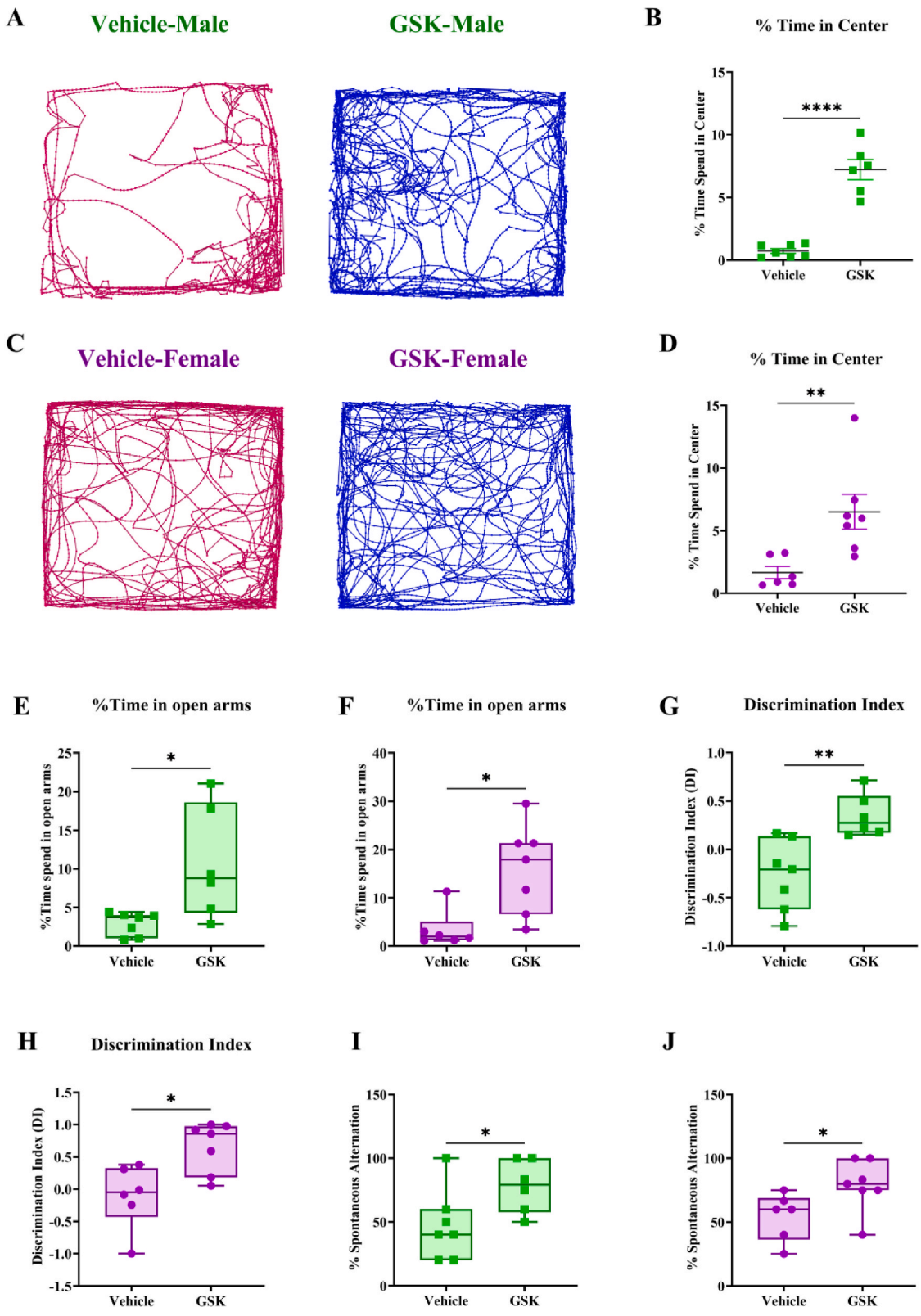

Fig. 6. Behavioral assessment following 2 weeks, post GSK therapy after SE.
(A, C) Representative open field tracking paths of vehicle (red) and GSK (blue) treated male (A) and female (C) animals. Male and female groups are denoted by green and purple color, respectively. Open field test: Percentage time spend in center by male (B), and female (D) animals. Elevated plus maze test: Percentage time spend in open arm by male (E) and female (F) animals. Novel object recognition test: Discrimination Index in male (G) and in female (H) animals. T-maze spontaneous alternation test: Percentage spontaneous alteration in male (I) and female (J) animals. n = 13 animals per sex-cohort, where n = 7, 6 and n = 6, 7 males and females, respectively; in vehicle and GSK-treated group, respectively. Data are presented as mean ± s.e.m. Statistical significance was determined by unpaired *t*-test. *p < 0.05, **p < 0.01, ****p < 0.0001, ns: not significant.

respectively) indicating their poor working memory. However, following GSK therapy animals achieved higher rate of successful alteration in both GSK treated male and female cohorts (Fig. 6I–J, respectively), suggesting that early treatment of GSK following SE prevents associated cognitive declines.

3.7. Prolong effect of GSK therapy on oxidative DNA damage at the early chronic phase of epilepsy

To determine whether early inhibition of seizure activity by GSK therapy confers sustained protection against oxidative DNA damage, we examined hippocampal tissue at the end of the 12-week vECoG monitoring period (Fig. 1; Group 2). Persistent oxidative stress and DNA damage have been implicated in the progression of epileptogenesis and chronic epilepsy, contributing to ongoing neuronal dysfunction and cognitive decline [55]. By assessing oxidative damage at this delayed time point, we sought to determine how ongoing seizure activity influences redox imbalance in both male and female animals, and to evaluate whether early NOX2 inhibition with GSK provides lasting neuroprotection against spontaneous seizure-induced oxidative injury.

In vehicle treated males, higher 8-OHdG (marker of DNA oxidation) fluorescence intensity was observed in the CA1 and CA3 subfields compared to GSK treated males, indicating increased oxidative damage in the hippocampus associated with greater levels of recurrent spontaneous seizures (Supp Fig. 6). This suggests that chronic seizure activity contributes to sustained oxidative stress, which can be mitigated by targeting NOX2 during the early phase of epilepsy development. However, we did not observe any significant differences in the CA1 and CA3 subfields between vehicle and GSK treated female animals (Supp Fig. 7), indicating that GSK treatment failed to exert a prolonged protective effect in females. These findings suggest that sex dependent differences in recurrent seizure activity at the early chronic phase, as well as limited involvement of NOX2 driven oxidative stress in female epilepsy pathophysiology, may contribute to the observed differences in GSK therapy outcomes between male and female animals.

3.8. Sustained neuroprotection by early GSK therapy during the chronic phase of epilepsy

To further evaluate the long-term neuroprotective potential of early NOX2 inhibition, we assessed neuronal integrity in the hippocampus at the 12th week following SE (Fig. 1; Group 2). This approach enabled us to determine whether an initial two week intervention with GSK could provide sustained protection against seizure induced neuronal loss during the early chronic phase of epilepsy.

In male animals, vehicle treated groups exhibit significantly higher neuronal death in the CA1 (Supp Fig. 8A and B) and CA3 (Supp Fig. 8A and C) subfields of hippocampus at 12 weeks. In contrast, males that received GSK therapy in the early post-SE period demonstrated preserved neuronal integrity in these regions, indicating that early GSK intervention provides a prolonged neuroprotective effect by reducing recurrent seizure activity over the course of vECoG monitoring (Supp Fig. 3A and B). In females, vehicle treated animals also showed evidence of neuronal death in the CA1 (Supp Fig. 9A and B) and CA3 (Supp Fig. 9A and C) subfields at 12 weeks. However, GSK treatment only partially protected against neuronal loss in the CA1 and failed to confer a significant prolonged effect in the CA3 region. These findings suggest that, while GSK therapy can provide some neuroprotection in females, its efficacy is reduced relative to males, particularly in the CA3 subfield. Altogether, these results highlight clear sex-dependent differences in the long-term neuroprotective effects of GSK therapy. The differential outcomes observed between males and females may reflect underlying complexities in seizure pathophysiology or the involvement of additional, sex specific mechanisms influencing neuronal vulnerability and therapeutic response.

4. Discussion

This study is the first, to our knowledge, to evaluate the disease modifying effects of the selective NOX2 inhibitor (GSK2795039) when administered immediately after SE, with long-term video-ECoG monitoring and behavioral follow up. We identify a critical post-SE therapeutic window and demonstrated that early inhibition of NOX2 effectively reduces seizure burden, neuronal damage, and oxidative stress, with sex specific differences in treatment response. These results not only support the pathogenic role of NOX2 derived ROS in epileptogenesis but also highlight the therapeutic potential of targeting redox signaling pathways immediately after SE.

Accumulating evidence implicates oxidative stress and neuroinflammation as key contributors to seizure propagation and treatment resistance [51,75–77]. Although NOX2 derived ROS is well-established in mediating oxidative damage and inflammation in neurological disorders like epilepsy [1,16,78–80]. Most available NOX inhibitors lack isoform selectivity [81–83], complicating the evaluation of NOX2 specific effects. GSK2795039 offers selective NOX2 inhibition with improved oral bioavailability, blood brain barrier permeability, and pharmacodynamic properties [83,84], avoiding the off target issues of non-selective inhibitors such as DPI, apocynin, or VAS2870 [82–84]. Pharmacokinetic studies of GSK2795039 have reported a plasma half-life of ~2 h in rats and ~12 min in mice following intravenous administration, with moderate brain penetration (brain:blood ratios of ~0.83 in rats and ~0.49 in mice) [84]. The compound exhibits relatively high clearance rates and variable oral bioavailability across species [84], characteristics that support its use for short-term, in vivo NOX2 inhibition in preclinical models. We previously employed the peptide-based inhibitor gp91ds-tat to examine NOX2 inhibition in chronic epilepsy [8], but the effects of early NOX2 inhibition after status epilepticus, particularly on cognitive deficits, epileptogenesis, and sex-dependent responses, remain underexplored. While sex differences in seizure susceptibility and treatment outcomes are recognized, the underlying NOX2-specific mechanisms are still not well understood [18,85–87].

We recently confirmed the promising candidacy of GSK2795039 in an in vitro epileptiform activity model, as well as its anticonvulsant efficacy in vivo, where we observed that pre-inhibition of NOX2 with GSK2795039 reduced PTZ-induced seizure susceptibility in animal models [88]. Building on our recent preliminary findings, the present study systematically investigated the therapeutic potential of GSK2795039 in targeting NOX2-derived ROS associated with oxidative DNA damage, neuroinflammation, and neuronal death following the initial insult by SE in the early phase of epileptogenesis (Fig. 1; Group 1). We further extended our investigation by monitoring the long term effects of early GSK2795039 intervention following SE on epilepsy development and seizure burden (Fig. 1; Group 2). By incorporating sex based analyses, this study offers novel insights into the role of NOX2 inhibition in epilepsy and underscores the potential influence of sex on therapeutic outcomes. Additionally, we demonstrated the protective efficacy of GSK2795039 against epilepsy associated cognitive deficits and its sustained neuroprotective effects in early chronic phase. Collectively, this study contributes to the growing evidence that NOX2 inhibition could serve as an effective strategy for reducing oxidative stress-induced neuronal excitability and epileptogenesis [39,89,90].

Early GSK treatment suppressed the SE induced neuroinflammation by reducing pro-inflammatory cytokines IL-6, IL-1β, and TNFα (Fig. 2A–C; 2I–K) while restoring the anti-inflammatory cytokine IL-10 (Fig. 2D; 2 L, respectively) in hippocampus and cortex, supporting the link between NOX2 activity, oxidative stress, and inflammatory signaling [43]. Interestingly, we investigate sex dependent variations in cytokine expression, particularly in IL-10 regulation, suggesting that females may employ a brain-region specific alternative anti-inflammatory pathways in response to SE. This aligns with previous reports showing sex specific immune responses in neurological

disorders, where females exhibit greater resilience to oxidative stress-induced damage owing to higher baseline levels of endogenous antioxidants and anti-inflammatory molecules [91]. Our study further revealed that NOX2 inhibition mitigated SE-induced oxidative DNA damage, particularly in male hippocampal neurons (Fig. 3A–D), which was significantly reduced by GSK treatment. In contrast, females exhibited a different pattern, with relatively lower 8-OHdG intensity (marker of DNA oxidation) in vehicle treated animals but pronounced neuronal loss and structural disruption in the CA1 and CA3 subfields, as evident from both 8-OHdG immunostaining (Fig. 3E–F) and Nissl staining (Fig. 4D). While these results suggest sex-specific differences in oxidative stress responses, it is important to note that 8-OHdG reflects only DNA oxidation and may not capture other forms of oxidative injury, such as lipid or protein oxidation. Therefore, the apparent lack of oxidative DNA damage in females does not rule out NOX2 activation or alternative oxidative mechanisms. To address this limitation, future studies will incorporate additional oxidative stress markers, including lipid peroxidation and glutathione redox balance, to better characterize redox dynamics during epileptogenesis in both sexes. Such markers will also help mechanistically distinguish NOX2 dependent from NOX2-independent effects; for instance, lipid peroxidation products (e.g., 4-HNE, MDA) can arise from mitochondrial or other non-NOX2 ROS sources, whereas alterations in glutathione redox status reflect the cell's overall antioxidant buffering capacity and may indicate compensatory pathways activated independently of NOX2 activity. Previous studies have shown that females generally possess higher baseline antioxidant capacity, including greater superoxide dismutase and catalase activity, lower baseline lipid peroxidation markers, and region specific antioxidant expression in the brain [7,87,92–98]. In addition, estrogen and other sex hormones modulate oxidative stress responses, with estrogen receptor beta (ERβ) mediated Nrf2 activation upregulating cytoprotective genes such as heme oxygenase-1 (HO-1) and NAD(P)H quinone oxidoreductase 1 (NQO1), enhancing glutathione synthesis, reducing lipid peroxidation, and improving mitochondrial resilience under oxidative stress [99–102]. Such estrogen-driven antioxidant mechanisms may partly explain the lower baseline oxidative damage and higher resistance to NOX2 derived ROS observed in females, potentially diminishing the relative impact of NOX2 inhibition in our model.

Beyond sex dependent biochemical responses, we further evaluated the overall therapeutic effects of GSK2795039 on seizure development and progression. Our randomized preclinical study revealed that GSK treatment significantly reduced seizure frequency and burden during epileptogenesis (Fig. 5A–C; Supp Fig. 3). This effect was more pronounced in males (92 ± 20 vs. 15 ± 5 seizures in vehicle vs. GSK-treated groups, respectively; Supp Fig. 3B) than in females (47 ± 13 vs. 10 ± 3; Supp Fig. 3D) over 12 weeks of vECoG monitoring. Notably, vehicle-treated males displayed a progressive increase in spontaneous seizure activity from the 8th week onward (Supp Fig. 2), suggesting stronger NOX2 involvement in male epileptogenesis. This sex disparity likely underpins the greater therapeutic impact of GSK in males and aligns with prior studies indicating that males are more vulnerable to NOX2-derived oxidative stress in various neuropathologies [23,25,103–106]. The observed long-term seizure suppression following early GSK treatment supports its disease-modifying potential. We previously demonstrated similar benefits using the NOX2-selective peptide inhibitor gp91ds-tat in chronic epilepsy models [8]. Additionally, GSK treatment reduced interictal spike frequency (Fig. 5J), indicating a broader impact on neuronal hyperexcitability. These findings reinforce the link between oxidative stress, inflammation, and epileptogenesis, consistent with reports that NOX2-generated ROS amplifies excitability and promotes seizure progression [17,107].

We also assessed cognitive outcomes and observed sex specific differences. GSK treated males exhibited significant improvements in locomotor activity (Supp Fig. 5A–D), reduced anxiety-like behavior (Fig. 6A–B, E; Supp Fig. 5I), and enhanced memory performance (Fig. 6G–I) compared to vehicle controls. These benefits may reflect males' lower baseline antioxidant capacity, making them more responsive to NOX2 inhibition. In contrast, females displayed more limited cognitive improvements, consistent with the previously described higher endogenous antioxidant defenses and hormonal modulation of redox pathways.

Additionally, the long-term neuroprotective effects of GSK2795039 were evident in vECoG monitored animals, where treated males showed a sustained reduction in hippocampal oxidative DNA damage (Supp Fig. 6), suggesting that early NOX2 inhibition can mitigate the cumulative oxidative burden associated with recurrent seizures [108]. In contrast, female GSK treated animals did not show significant changes compared to vehicle controls (Supp Fig. 7), further supporting the earlier observation that alternative, NOX2 independent antioxidant mechanisms may predominate in females.

Collectively, our findings identify NOX2 as a key mediator of seizure-induced oxidative stress and neuroinflammation, with GSK2795039 showing strong potential to counter epileptogenesis. The pronounced efficacy in males underscores the need for sex specific therapeutic approaches and for exploring alternative antioxidant and neuroprotective mechanisms in females. Key translational challenges remain, including the absence of clinically approved, isoform selective NOX2 inhibitors and specific in vivo biomarkers to distinguish direct NOX2 activity from downstream or compensatory effects. Future work should leverage genetic models, such as NOX2 knockouts or cell type specific deletions, alongside the development of brain penetrant, isoform selective inhibitors with improved safety profiles. Such advances, combined with sex-stratified study designs, will be essential to refine redox targeted strategies for epilepsy prevention and treatment.

5. Conclusion

This study demonstrates that early pharmacological inhibition of NOX2 using GSK2795039 provides sustained neuroprotective effects in a rat model of epilepsy, including reductions in seizure burden, oxidative stress, neuroinflammation, and cognitive impairments. Importantly, the therapeutic response differed by sex, with male rats showing greater benefit, likely due to their lower baseline antioxidant defenses and higher vulnerability to NOX2 mediated oxidative damage. In contrast, females may rely more on alternative antioxidant and inflammatory pathways, indicating that combination or adjunctive therapies may be necessary for optimal benefit. These findings underscore the need to incorporate sex specific mechanisms when designing personalized treatment strategies for epilepsy. While our data support NOX2 as a promising therapeutic target, especially for redox vulnerable populations, future research should include broader assessments of oxidative damage and explore NOX2 independent mechanisms, particularly in females. Overall, our findings support the potential of redox-targeted interventions to modify epileptogenesis and improve long-term outcomes after status epilepticus.

CRediT authorship contribution statement

Prince Kumar Singh: Writing – review & editing, Writing – original draft, Visualization, Methodology, Investigation, Formal analysis, Conceptualization. **Shweta Maurya:** Writing – review & editing, Methodology, Investigation, Formal analysis. **Aseel Saadi:** Writing – review & editing, Methodology, Investigation. **Taige Zhang:** Methodology, Formal analysis. **Andreas Lieb:** Writing – review & editing, Methodology. **Tawfeeq Shekh-Ahmad:** Writing – review & editing, Writing – original draft, Visualization, Supervision, Project administration, Funding acquisition, Formal analysis, Conceptualization.

Ethics approval

All animal experiments were performed in compliance with the guidelines of the Association for Assessment and Accreditation of

Laboratory Animal Care International and were approved by the Institutional Animal Care and Use Committee (IACUC) of the Hebrew University of Jerusalem (Protocol Code: MD-20-16,254-5; Approval Date: July 13, 2020).

Consent for publication

All authors have read and approved the final manuscript for publication.

Data availability statement

The data supporting the findings of this study are available from the corresponding author upon reasonable request.

Funding

This research was funded in whole or in part by The Israel Science Foundation (grant no. 1976/20 to TSA) and the Ministry of Science and Technology, Israel (grant no. 5100 to TSA); the Austrian Science Fund (FWF) grants 10.55776/P33222 and 10.55776/P35579 to AL.

Declaration of competing interest

The authors declare that they have no known competing financial interests or personal relationships that could have appeared to influence the work reported in this paper.

Acknowledgements

The authors gratefully acknowledge the generous support of The Neubauer Family Foundation. Financial support from the David R. Bloom Center for Pharmacy is also sincerely appreciated.

This work is abstracted from the PhD thesis of Mr. Prince Kumar Singh, submitted in partial fulfillment of the requirements for the PhD degree at The Hebrew University of Jerusalem.

Appendix A. Supplementary data

Supplementary data to this article can be found online at https://doi.org/10.1016/j.redox.2025.103830.

Data availability

Data will be made available on request.

References

[1] M. Patel, Targeting oxidative stress in central nervous system disorders, Trends Pharmacol. Sci. 37 (9) (2016) 768–778.
[2] S. Rowley, M. Patel, Mitochondrial involvement and oxidative stress in temporal lobe epilepsy, Free Radic. Biol. Med. 62 (2013) 121–131.
[3] A. Pauletti, et al., Targeting oxidative stress improves disease outcomes in a rat model of acquired epilepsy, Brain 142 (7) (2019) e39.
[4] A.M. Brennan, et al., NADPH oxidase is the primary source of superoxide induced by NMDA receptor activation, Nat. Neurosci. 12 (7) (2009) 857–863.
[5] K. Bedard, K.H. Krause, The NOX family of ROS-generating NADPH oxidases: physiology and pathophysiology, Physiol. Rev. 87 (1) (2007) 245–313.
[6] S. Kovac, A. Dinkova-Kostova, A. Abramov, The role of reactive oxygen species in epilepsy, React. Oxygen Species 1 (1) (2016).
[7] A. Saadi, et al., Spatial, temporal, and cell-type-specific expression of NADPH Oxidase isoforms following seizure models in rats, Free Radic. Biol. Med. 190 (2022) 158–168.
[8] P.K. Singh, et al., Specific inhibition of NADPH oxidase 2 modifies chronic epilepsy, Redox Biol. 58 (2022) 102549.
[9] E.J. Shin, et al., Role of oxidative stress in epileptic seizures, Neurochem. Int. 59 (2) (2011) 122–137.
[10] A. Vezzani, et al., The role of inflammation in epilepsy, Nat. Rev. Neurol. 7 (1) (2011) 31–40.
[11] K. Strle, et al., Interleukin-10 in the brain, Crit. Rev. Immunol. 21 (5) (2001) 427–449.
[12] A.L.M. Parsons, et al., The interconnected mechanisms of oxidative stress and neuroinflammation in epilepsy, Antioxidants (Basel) 11 (1) (2022).
[13] H.M. Gao, H. Zhou, J.S. Hong, NADPH oxidases: novel therapeutic targets for neurodegenerative diseases, Trends Pharmacol. Sci. 33 (6) (2012) 295–303.
[14] P. Mander, G.C. Brown, Activation of microglial NADPH oxidase is synergistic with glial iNOS expression in inducing neuronal death: a dual-key mechanism of inflammatory neurodegeneration, J. Neuroinflammation 2 (2005) 20.
[15] H.M. Gao, et al., Synergistic dopaminergic neurotoxicity of the pesticide rotenone and inflammogen lipopolysaccharide: relevance to the etiology of Parkinson's disease, J. Neurosci. 23 (4) (2003) 1228–1236.
[16] T. Shekh-Ahmad, et al., Combination antioxidant therapy prevents epileptogenesis and modifies chronic epilepsy, Redox Biol. 26 (2019) 101278.
[17] A. Malkov, et al., Activation of nicotinamide adenine dinucleotide phosphate oxidase is the primary trigger of epileptic seizures in rodent models, Ann. Neurol. 85 (6) (2019) 907–920.
[18] C.A. Christian, et al., Sex differences in the epilepsies and associated comorbidities: implications for use and development of pharmacotherapies, Pharmacol. Rev. 72 (4) (2020) 767–800.
[19] D.S. Reddy, Sex differences in the anticonvulsant activity of neurosteroids: sex differences in anticonvulsant neurosteroids, J. Neurosci. Res. 95 (2017) 661–670.
[20] H.E. Scharfman, N.J. MacLusky, Sex differences in the neurobiology of epilepsy: a preclinical perspective, Neurobiol. Dis. 72 (2014) 180–192.
[21] N. Sumien, et al., Neurodegenerative disease: roles for sex, hormones, and oxidative stress, Endocrinology 162 (11) (2021) bqab185.
[22] A.A. Miller, et al., Effect of gender and sex hormones on vascular oxidative stress, Clin. Exp. Pharmacol. Physiol. 34 (10) (2007) 1037–1043.
[23] J. Barp, et al., Myocardial antioxidant and oxidative stress changes due to sex hormones, Braz. J. Med. Biol. Res. 35 (9) (2002) 1075–1081.
[24] K. Bhatia, et al., Oxidative stress contributes to sex differences in angiotensin II-mediated hypertension in spontaneously hypertensive rats, Am. J. Physiol. Regul. Integr. Comp. Physiol. 302 (2) (2012) R274–R282.
[25] M.C. Kander, Y. Cui, Z. Liu, Gender difference in oxidative stress: a new look at the mechanisms for cardiovascular diseases, J. Cell Mol. Med. 21 (5) (2017) 1024–1032.
[26] R.J. Racine, Modification of seizure activity by electrical stimulation. II. Motor seizure, Electroencephalogr. Clin. Neurophysiol. 32 (3) (1972) 281–294.
[27] M.W. Pfaffl, A new mathematical model for relative quantification in real-time RT-PCR, Nucleic Acids Res. 29 (9) (2001) e45.
[28] T. Nath, et al., Using DeepLabCut for 3D markerless pose estimation across species and behaviors, Nat. Protoc. 14 (7) (2019) 2152–2176.
[29] G. Li, et al., Cytokines and epilepsy, Seizure 20 (3) (2011) 249–256.
[30] C. Eriksson, et al., Increased expression of mRNA encoding interleukin-1β and caspase-1, and the secreted isoform of interleukin-1 receptor antagonist in the rat brain following systemic kainic acid administration, J. Neurosci. Res. 60 (2) (2000) 266–279.
[31] M. Rizzi, et al., Glia activation and cytokine increase in rat hippocampus by kainic acid-induced status epilepticus during postnatal development, Neurobiol. Dis. 14 (3) (2003) 494–503.
[32] K. Lehtimäki, et al., Expression of cytokines and cytokine receptors in the rat brain after kainic acid-induced seizures, Mol. Brain Res. 110 (2) (2003) 253–260.
[33] F. Dhote, et al., Prolonged inflammatory gene response following soman-induced seizures in mice, Toxicology 238 (2–3) (2007) 166–176.
[34] C.R. Plata-Salamán, et al., Kindling modulates the IL-1β system, TNF-α, TGF-β1, and neuropeptide mRNAs in specific brain regions, Mol. Brain Res. 75 (2) (2000) 248–258.
[35] T.K. Lin, et al., Seizure-induced oxidative stress in status epilepticus: is antioxidant Beneficial? Antioxidants (Basel) 9 (11) (2020).
[36] J. Kalita, et al., Oxidative stress in status epilepticus: a clinical-radiological correlation, Brain Res. 1704 (2019) 85–93.
[37] T. Shekh-Ahmad, et al., Reactive oxygen species in status epilepticus, Epilepsy Behav. 101 (2019) 106410.
[38] T. Foiadelli, et al., Neuroinflammation and status epilepticus: a narrative review unraveling a complex interplay, Front. Pediatr. 11 (2023) 1251914.
[39] K.K. Borowicz-Reutt, S.J. Czuczwar, Role of oxidative stress in epileptogenesis and potential implications for therapy, Pharmacol. Rep. 72 (5) (2020) 1218–1226.
[40] T. Fabisiak, M. Patel, Crosstalk between neuroinflammation and oxidative stress in epilepsy, Front. Cell Dev. Biol. 10 (2022) 976953.
[41] A. Kumar, et al., NOX2 drives M1-like microglial/macrophage activation and neurodegeneration following experimental traumatic brain injury, Brain Behav. Immun. 58 (2016) 291–309.
[42] D. Tu, et al., Activation of neuronal NADPH oxidase NOX2 promotes inflammatory neurodegeneration, Free Radic. Biol. Med. 200 (2023) 47–58.
[43] C. Almeida, et al., Distinct cell-specific roles of NOX2 and MyD88 in epileptogenesis, Front. Cell Dev. Biol. 10 (2022) 926776.
[44] H.-M. Wu, W.-Y. Huang, Role of NOX2 in seizure susceptibility of mice following systemic inflammation (P4.251), Neurology 84 (14_supplement) (2015). P4.251.
[45] A. Vezzani, et al., IL-1 receptor/Toll-like receptor signaling in infection, inflammation, stress and neurodegeneration couples hyperexcitability and seizures, Brain Behav. Immun. 25 (7) (2011) 1281–1289.
[46] A.M. Franchini, et al., FcgammaR-driven release of IL-6 by macrophages requires NOX2-dependent production of reactive oxygen species, J. Biol. Chem. 288 (35) (2013) 25098–25108.
[47] W.Y. Huang, et al., NADPH oxidases as potential pharmacological targets against increased seizure susceptibility after systemic inflammation, J. Neuroinflammation 15 (1) (2018) 140.

[48] D. Bertoglio, et al., Kainic acid-induced post-status epilepticus models of temporal lobe epilepsy with diverging seizure phenotype and Neuropathology, Front. Neurol. 8 (2017) 588.
[49] E. Rusina, C. Bernard, A. Williamson, The kainic acid models of temporal lobe epilepsy, eneuro 8 (2) (2021). ENEURO.0337-20.2021.
[50] W. Loscher, C. Brandt, Prevention or modification of epileptogenesis after brain insults: experimental approaches and translational research, Pharmacol. Rev. 62 (4) (2010) 668–700.
[51] A. Vezzani, S. Balosso, T. Ravizza, Neuroinflammatory pathways as treatment targets and biomarkers in epilepsy, Nat. Rev. Neurol. 15 (8) (2019) 459–472.
[52] S. Puttachary, et al., Seizure-induced oxidative stress in temporal lobe epilepsy, BioMed Res. Int. 2015 (2015) 745613.
[53] A. Behrouzi, M.R. Kelley, J.C. Fehrenbacher, Oxidative DNA damage: a role in altering neuronal function, J. Cell Signal 3 (3) (2022) 160–166.
[54] M. Patel, A metabolic paradigm for epilepsy, Epilepsy Curr. 18 (5) (2018) 318–322.
[55] S. Waldbaum, M. Patel, Mitochondrial dysfunction and oxidative stress: a contributing link to acquired epilepsy? J. Bioenerg. Biomembr. 42 (6) (2010) 449–455.
[56] A. Valavanidis, T. Vlachogianni, C. Fiotakis, 8-hydroxy-2′-deoxyguanosine (8-OHdG): a critical biomarker of oxidative stress and carcinogenesis, J. Environ. Sci. Health Part C 27 (2) (2009) 120–139.
[57] M. Bogdanov, et al., Increased oxidative damage to DNA in ALS patients, Free Radic. Biol. Med. 29 (7) (2000) 652–658.
[58] Y. Ihara, et al., Oxidative stress and metal content in blood and cerebrospinal fluid of amyotrophic lateral sclerosis patients with and without a Cu, Zn-superoxide dismutase mutation, Neurol. Res. 27 (1) (2005) 105–108.
[59] P. Fitzmaurice, et al., Evidence for DNA damage in amyotrophic lateral sclerosis, Muscle Nerve 19 (6) (1996) 797–798.
[60] R.J. Ferrante, et al., Evidence of increased oxidative damage in both sporadic and familial amyotrophic lateral sclerosis, J. Neurochem. 69 (5) (1997) 2064–2074.
[61] E. Niedzielska, et al., Oxidative stress in neurodegenerative diseases, Mol. Neurobiol. 53 (2016) 4094–4125.
[62] P.J. McKinnon, Maintaining genome stability in the nervous system, Nat. Neurosci. 16 (11) (2013) 1523–1529.
[63] M. Sashindranath, et al., Early hippocampal oxidative stress is a direct consequence of seizures in the rapid electrical amygdala kindling model, Epilepsy Res. 90 (3) (2010) 285–294.
[64] S.G. Jarrett, et al., Mitochondrial DNA damage and impaired base excision repair during epileptogenesis, Neurobiol. Dis. 30 (1) (2008) 130–138.
[65] M. Méndez-Armenta, et al., Oxidative stress associated with neuronal apoptosis in experimental models of epilepsy, Oxid. Med. Cell. Longev. 2014 (2014) 293689.
[66] X.-Y. Mao, H.-H. Zhou, W.-L. Jin, Redox-related neuronal death and crosstalk as drug targets: focus on epilepsy, Front. Neurosci. 13 (2019) 512.
[67] L. Narciso, et al., The response to oxidative DNA damage in neurons: mechanisms and disease, Neural Plast. 2016 (2016) 3619274.
[68] K.J. Staley, F.E. Dudek, Interictal spikes and epileptogenesis, Epilepsy Curr. 6 (6) (2006) 199–202.
[69] M. de Curtis, G. Avanzini, Interictal spikes in focal epileptogenesis, Prog. Neurobiol. 63 (5) (2001) 541–567.
[70] W. Löscher, C.E. Stafstrom, Epilepsy and its neurobehavioral comorbidities: insights gained from animal models, Epilepsia 64 (1) (2023) 54–91.
[71] G.L. Holmes, Cognitive impairment in epilepsy: the role of network abnormalities, Epileptic Disord. 17 (2) (2015) 101–116.
[72] A. Novak, K. Vizjak, M. Rakusa, Cognitive impairment in people with epilepsy, J. Clin. Med. 11 (1) (2022).
[73] A. Kandlur, K. Satyamoorthy, G. Gangadharan, Oxidative stress in cognitive and epigenetic aging: a retrospective glance, Front. Mol. Neurosci. 13 (2020) 41.
[74] C.C. Aguiar, et al., Oxidative stress and epilepsy: literature review, Oxid. Med. Cell. Longev. 2012 (2012) 795259.
[75] J. Shi, et al., The role of neuroinflammation and network anomalies in drug-resistant epilepsy, Neurosci. Bull. (2025) 1–25.
[76] N. Cardenas-Rodriguez, et al., Role of oxidative stress in refractory epilepsy: evidence in patients and experimental models, Int. J. Mol. Sci. 14 (1) (2013) 1455–1476.
[77] W. Loscher, et al., Drug resistance in epilepsy: clinical impact, potential mechanisms, and new innovative treatment options, Pharmacol. Rev. 72 (3) (2020) 606–638.
[78] M. Patel, et al., Activation of NADPH oxidase and extracellular superoxide production in seizure-induced hippocampal damage, J. Neurochem. 92 (1) (2005) 123–131.
[79] J.N. Pearson, et al., Reactive oxygen species mediate cognitive deficits in experimental temporal lobe epilepsy, Neurobiol. Dis. 82 (2015) 289–297.
[80] S. Kovac, et al., Seizure activity results in calcium- and mitochondria-independent ROS production via NADPH and xanthine oxidase activation, Cell Death Dis. 5 (10) (2014) e1442.
[81] M.E. Cifuentes-Pagano, D.N. Meijles, P.J. Pagano, Nox inhibitors & therapies: rational design of peptidic and small molecule inhibitors, Curr. Pharm. Des. 21 (41) (2015) 6023–6035.
[82] F. Augsburger, et al., Pharmacological characterization of the seven human NOX isoforms and their inhibitors, Redox Biol. 26 (2019) 101272.
[83] L. Hou, et al., Nicotinamide adenine dinucleotide phosphate oxidase and neurodegenerative diseases: mechanisms and therapy, Antioxidants Redox Signal. 33 (5) (2020) 374–393.
[84] K. Hirano, et al., Discovery of GSK2795039, a novel small molecule NADPH oxidase 2 inhibitor, Antioxidants Redox Signal. 23 (5) (2015) 358–374.
[85] M.F. Hammer, et al., Sex differences in physiological response to increased neuronal excitability in a knockin mouse model of pediatric epilepsy, Clin. Sci. (Lond.) 138 (4) (2024) 205–223.
[86] H.E. Scharfman, N.J. MacLusky, Sex differences in the neurobiology of epilepsy: a preclinical perspective, Neurobiol. Dis. 72 (2014) 180–192. Pt B.
[87] J.A. Ruszkiewicz, et al., Sex-specific differences in redox homeostasis in brain norm and disease, J. Mol. Neurosci. 67 (2) (2019) 312–342.
[88] P.K. Singh, et al., Targeting NOX2 mitigates seizure susceptibility, oxidative stress, and neuroinflammation in the pentylenetetrazol seizure model, Free Radic. Biol. Med. 235 (2025) 306–316.
[89] Y. Zilberter, D.R. Tabuena, M. Zilberter, NOX-induced oxidative stress is a primary trigger of major neurodegenerative disorders, Prog. Neurobiol. 231 (2023) 102539.
[90] P. Ambrogini, et al., Excitotoxicity, neuroinflammation and oxidant stress as molecular bases of epileptogenesis and epilepsy-derived neurodegeneration: the role of vitamin E, Biochim. Biophys. Acta Mol. Basis Dis. 1865 (6) (2019) 1098–1112.
[91] L.M. Ruiz-Perera, et al., NF-kappaB p65 directs sex-specific neuroprotection in human neurons, Sci. Rep. 8 (1) (2018) 16012.
[92] J. Vina, et al., Females live longer than males: role of oxidative stress, Curr. Pharm. Des. 17 (36) (2011) 3959–3965.
[93] G. Ehrenbrink, et al., Antioxidant enzymes activities and protein damage in rat brain of both sexes, Exp. Gerontol. 41 (4) (2006) 368–371.
[94] S. Sandouka, et al., Nrf2 is predominantly expressed in hippocampal neurons in a rat model of temporal lobe epilepsy, Cell Biosci. 13 (1) (2023) 3.
[95] S. Sandouka, et al., Nrf2 is expressed more extensively in neurons than in astrocytes following an acute epileptic seizure in rats, J. Neurochem. 165 (4) (2023) 550–562.
[96] J.I. Kitay, Sex differences in adrenal cortical secretion in the rat, Endocrinology 68 (5) (1961) 818–824.
[97] M. Weinstock, et al., Gender differences in sympathoadrenal activity in rats at rest and in response to footshock stress, Int. J. Dev. Neurosci. 16 (3–4) (1998) 289–295.
[98] E. Brunelli, et al., Sex differences in oxidative stress biomarkers, Curr. Drug Targets 15 (8) (2014) 811–815.
[99] I. Khan, et al., 17-β estradiol rescued immature rat brain against glutamate-induced oxidative stress and neurodegeneration via regulating Nrf2/HO-1 and MAP-kinase signaling pathway, Antioxidants 10 (6) (2021) 892.
[100] C. Zhu, et al., 17β-Estradiol up-regulates Nrf2 via PI3K/AKT and estrogen receptor signaling pathways to suppress light-induced degeneration in rat retina, Neuroscience 304 (2015) 328–339.
[101] P.K. Singh, T. Shekh-Ahmad, Nrf2 as a potential target for the treatment of epilepsy, Neural Regen. Res. 19 (9) (2024).
[102] M.A. Arevalo, I. Azcoitia, L.M. Garcia-Segura, The neuroprotective actions of oestradiol and oestrogen receptors, Nat. Rev. Neurosci. 16 (1) (2015) 17–29.
[103] T. Ide, et al., Greater oxidative stress in healthy young men compared with premenopausal women, Arterioscler. Thromb. Vasc. Biol. 22 (3) (2002) 438–442.
[104] A.A. Miller, et al., Effect of gender on NADPH-oxidase activity, expression, and function in the cerebral circulation: role of estrogen, Stroke 38 (7) (2007) 2142–2149.
[105] P. Matarrese, et al., Gender disparity in susceptibility to oxidative stress and apoptosis induced by autoantibodies specific to RLIP76 in vascular cells, Antioxidants Redox Signal. 15 (11) (2011) 2825–2836.
[106] M.E. Jung, D.B. Metzger, A sex difference in oxidative stress and behavioral suppression induced by ethanol withdrawal in rats, Behav. Brain Res. 314 (2016) 199–214.
[107] A. Malkov, et al., Abeta initiates brain hypometabolism, network dysfunction and behavioral abnormalities via NOX2-induced oxidative stress in mice, Commun. Biol. 4 (1) (2021) 1054.
[108] S. Petrillo, et al., Imbalance of systemic redox biomarkers in children with epilepsy: role of ferroptosis, Antioxidants (Basel) 10 (8) (2021) 1267.